2015

Design, Fabrication, and Testing of a Multi-Cycle Pulse Detonation Engine

Eli M. Thorpe

Design, Fabrication, and Testing of a Multi-Cycle Pulse Detonation Engine

Eli M. Thorpe

Thesis submitted to the
College of Engineering and Mineral Resources
at West Virginia University
in partial fulfillment of the requirements
for the degree of

Masters
in
Mechanical Engineering

Patrick H. Browning, Ph.D., Chair
Andrew C. Nix, Ph.D.
V'yacheslav Akkerman, Ph.D.

Department of Mechanical and Aerospace Engineering

Morgantown, West Virginia
2015

Keywords: Pulse Detonation Engine, Multi-Cycle, Multi-Fuel

ABSTRACT

Design, Fabrication, and Testing of a Multi-Cycle Pulse Detonation Engine

Eli M. Thorpe

With the constant drive to improve the efficiency of systems used to generate heat and work pulse detonation engines have been explored. Pulse detonation engines can be described by the Humphrey thermodynamic cycle which, in theory, has advantages over the Brayton, Otto, and Diesel cycles.

This work is concerned with the design, fabrication, and the initial tests of a pulse detonation laboratory test bed. The test bed was designed with modularity and ease of alteration in mind while ensuring that a wide range of detonable fuel and oxidizer mixtures where able to be utilized.

Initial testing with a methane and oxygen mixture showed repeatable detonations in both single shot and cyclic operating modes. The expected detonation velocity was 2390m/s. Detonation was monitored with ionization probes and detonation velocities of 2391m/s were found as close as 30” from ignition source and some form of detonation as close as 6” from the ignition source.

Dedication

To my Mother, my Brother, and one so oft forgotten in these things, my Father.
To those who were there.
To those who could not be.
-Eli

Acknowledgements

There were more than a few people without which this project would not have come to fruition. Some have large and overarching roles while others filled more specific areas.

For my advisor, Dr. Browning, for the idea, direction, and in general being as close to an ideal advisor as I can imagine. While this may not seem like much, or take up much page space, it is very appreciated for the year and a half this project has been going on for.

For my brother, Justin Thorpe, who holds a masters in EE and specializes in motors and controls, for without those long and in depth conversations on EE the PDE would have been a lump of metal. Or a lot more expensive.

For my committee members, Dr. Akkerman and Dr. Nix, for being available and helpful whenever it was needed.

For the MAE machine shop overlord, Cliff, without whom I would not have had access to many of the machines needed to turn the raw materials into a PDE.

For the ever present Kelsey, without whom I could not have run my initial test firing when I did or accessed some of the facilities I needed to.

For my summer STEM SURE, Taylor, for that quite enjoyable summer blowing things up to make sure the detonation detector worked.

For all those others too…

Contents

List of Figures

List of Tables

Nomenclature

Abbreviations

BJT	Bipolar Junction Transistor
BR	Blockage Ratio
CAD	Computer Aided Design
CEA	Chemical Equilibrium with Applications
CJ	Chapman-Jouguet
COM	Communication
DAQ	Data Acquisition Unit
DDT	Detonation to Deflagration Transition
DIO	Digital Input Output
ID	Inner Diameter
IDE	Integrated Development Environment
MOSFET	Metal-Oxide-Semiconductor Field-Effect Transistors
PDE	Pulse Detonation Engine
PSIG	Pounds per Square Inch Gauge
PWM	Pulse width modulation
TNT	Trinitrotoluene
vs.	Versus
WVU	West Virginia University
ZND	Zel'dovich-Neumann-Doring

Symbols

A^*	*Sonic Throat Area*
C	*Constant*
E	*Energy*
g	*Gram*
H	*Inductance*
J	*Joule*
m	*Mass*
$\dot{m}$	*Mass Flow per Unit Time*
n	*Sample*
P	*Pressure*
q	*Specific Heat*
r	*Radius*
R_{spec}	*Specific Gas Constant*
s	*Specific Entropy*
s	*Second*
t	*Time*
T	*Temperature*
V	*Velocity*
$\forbidden{V}$	*Volume*
v	Voltage
v	*Specific Volume*
λ	*Cell Size*
η	*Thermal Efficiency*

Φ	*Fuel/Oxidizer Equivalence Ratio* $\frac{F_{fuel}/O_{ox}}{F_{stoich}}$
γ	*Specific heat ratio* $\frac{C_p}{C_v}$
ρ	*Density*
Ω	*Resistance*

Subscripts

0	*Total condition*
0psig	*At zero psig pressure*
1	*State 1*
2	*State 2*
3	*State 3*
Act	*Actual*
Br	*Brayton*
calc	*Calculated*
CJ	*Chapman-Jouguet condition*
exp	*Experimental*
Hm	*Humphrey*
mf	*Mass Flow*
Spec	*Specific*
Stoich	*Stoichiometric*

Chapter 1: Introduction

Background

General

Thermodynamic cycles with air as the working fluid are commonly used in propulsion and power production. Some commonly used cycles are the Brayton, Diesel, and Otto. These cycles are used to describe jet, Diesel, and gasoline engines respectively. Of recent and past interest is the Humphrey cycle which is used to describe a Pulse Detonation Engine (PDE). A PDE can be used for propulsion and energy conversion. Figure 1 shows an example of a PDE being used for propulsion with an experimental aircraft that was modified to use a several PDE's next to each other with the nearest being visible as the long tube extending from the rear of the plane.

Figure 1: Modified Rutan Long-EZ with PDE during January 31, 2008 test flight. Photo courtesy of Air Force Research Lab.

What makes the PDE, or other forms of detonation engines, desirable can be seen in Figure 2 which shows the pressure (P) – specific volume (v) and temperature (T) –

specific entropy (s) diagrams. These diagrams, in their most basic form, describe an idealized example of each particular thermodynamic cycle and the net work (P-v) or net heat (T-s) output shown by the area inside the cycle. In these diagrams it can be seen that the Humphrey cycle has an isochoric (i.e., constant volume) process from state 2 to 3 which gives it an advantage when compared to the Brayton and Diesel cycles as it increases the area inside the cycle. It also has an isobaric (i.e., constant pressure) process from state 4 to 1 which gives it an advantage over the Diesel and Otto cycles which also increases the area inside the cycle.

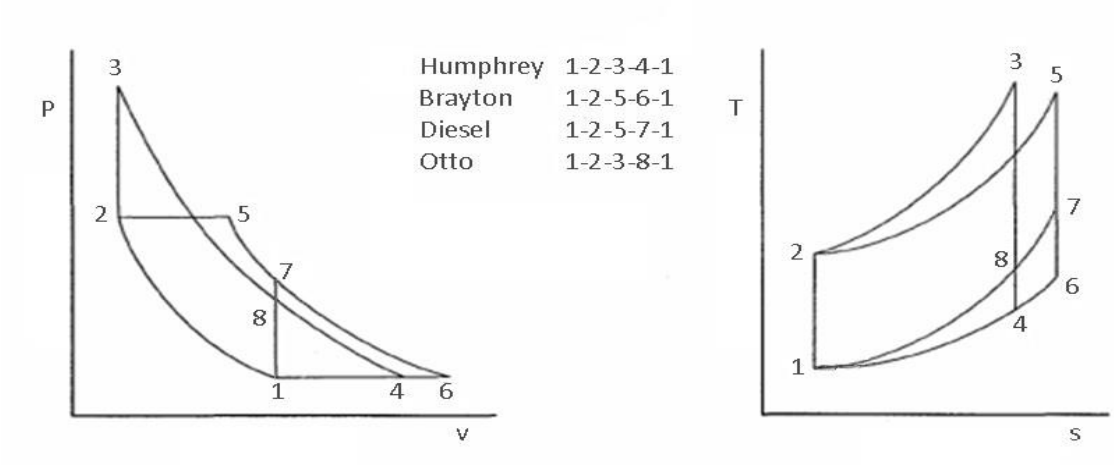

Figure 2: P-v and T-s Diagrams of Humphrey, Brayton, Diesel, and Otto cycles.

The Brayton, Diesel, and Otto cycles have in common that they rely on a combustion process known as deflagration. A deflagration is a type of combustion characterized by a flame which propagates through the combustible mixture at a speed that is subsonic relative to the medium the flame is propagating through. A deflagration's primary method of propagation is through heat transfer between molecules [1]. It is noteworthy to mention that while a deflagration is subsonic relative to the medium it passes through it could be supersonic relative to the an outside observer. However, the PDE, described by the Humphrey cycle, utilizes a combustion process known as

detonation. A detonation is a combustion process which can propagate very rapidly, at supersonic speeds relative to the medium it passes through and has an associated shockwave. In a detonation the primary means of propagation is from the associated shock wave [1].

Generally speaking, a detonation is capable of liberating more energy from a given mixture than deflagration. This can be seen in Figure 3 which compares the theoretical thermal efficiency of the Brayton and Humphrey cycle which have the same specific heat ratio (γ) and temperatures at state 1 and 2. The temperature at state 3 is varied. As can be seen in the figure, depending upon the combustor exit temperature, the ideal thermal efficiency increase is between 7% and 14%. The equations used for the

thermal efficiency of the Brayton cycle ($\eta_{\blacklozenge\blacklozenge}$) and Humphrey cycle ($\eta_{H\blacklozenge}$) are given in Equations 1 and 2.

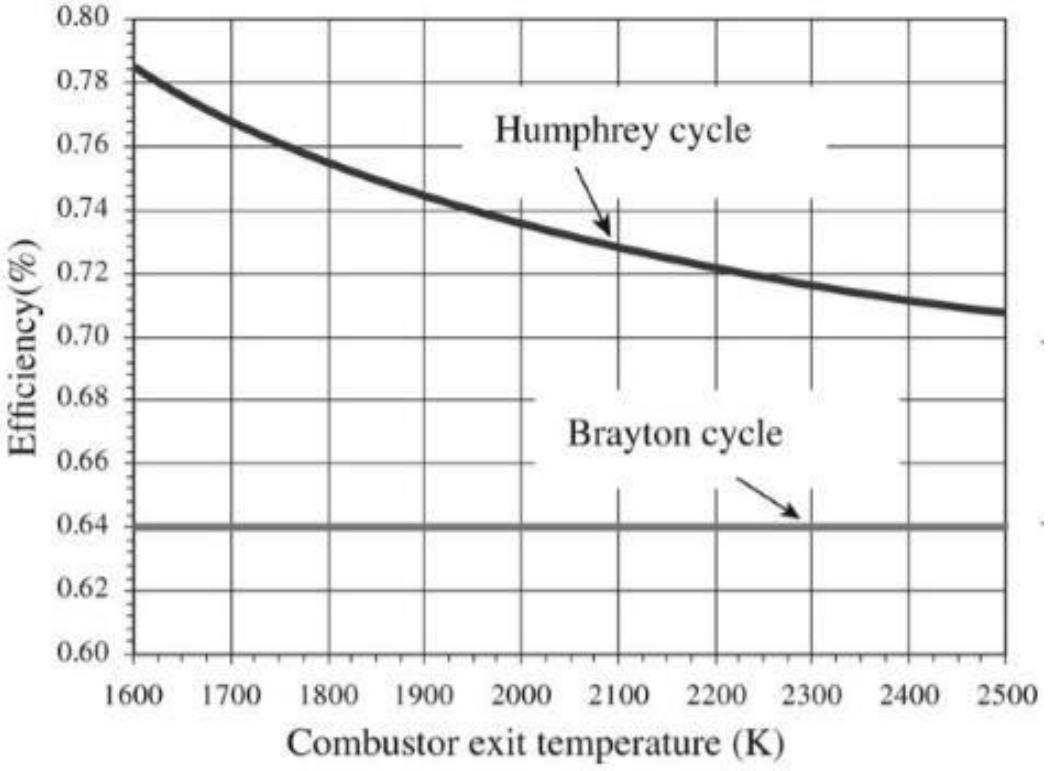

Figure 3: Ideal thermal efficiency of Humphrey and Brayton cycles for γ = 1.4, and T_1 = 288 K, T_2 = 800 K, and T_3 that varies between 1600 and 2500 K [2].

$$\eta_{\square\square} = 1 - \frac{\square}{\square} \qquad \textbf{Eqn. 1}$$

$$_{H\square}\eta = 1 - \gamma(\frac{\square}{\square})\frac{(\frac{\square}{\square})^{\frac{+}{\gamma}-1}}{(\frac{\square}{\square})-1} \qquad \textbf{Eqn. 2}$$

It is noted in Rodriguez [3] that, "[t]his theoretical efficiency improvement may be translated into a specific impulse performance measure improvement of how efficiently the engine converts propellant into useful thrust keeping in mind that this is only an approximation of ideal cycles." This theoretical increase in thermal efficiency and its effect on thrust and specific impulse can be more easily seen in an experiment done by Frolov et al. [4]. In this experiment, a continuous detonation engine was operated

at various equivalence ratios (Φ), which is the ratio of the actual fuel to oxidizer ratio to

the stoichiometric fuel to oxidizer ratio, and collected data on the thrust and specific impulse. It was found that for the equivalence ratios that could support either mode of combustion that both the thrust and specific impulse were approximately 6-7% greater for the detonation mode. This is shown in Figure 4.

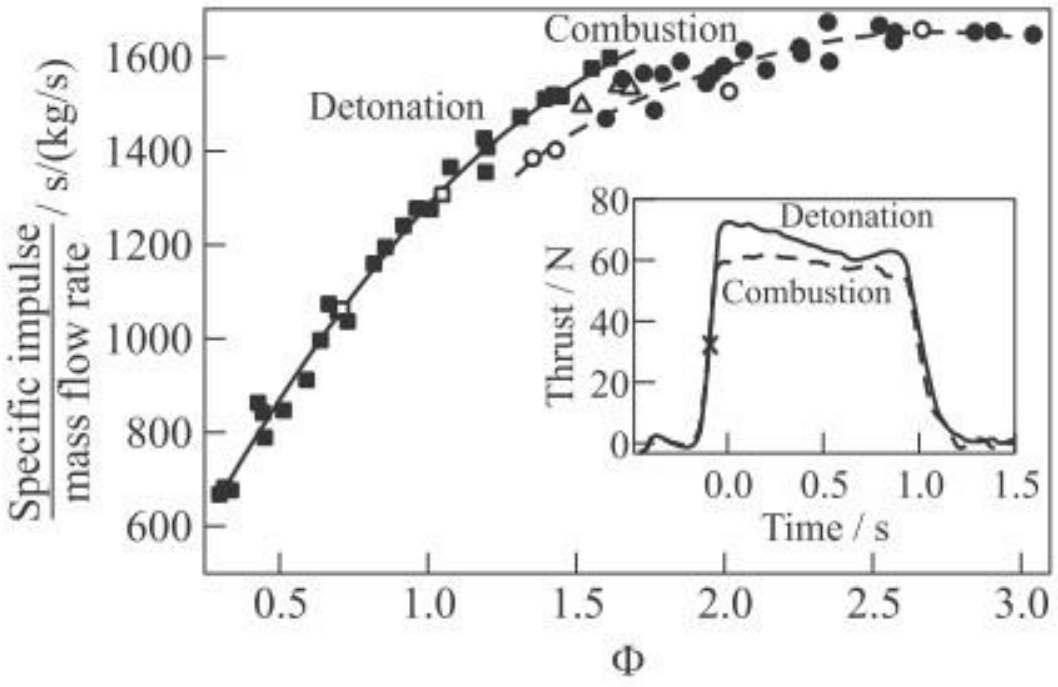

Figure 4: Specific Impulse per Mass Flow Rate vs. Equivalence Ratio [4].

A basic PDE can be seen as a tube with a closed end, some mechanism to fill the tube with a detonable mixture of fuel and oxidizer, and another mechanism to ignite the mixture. To achieve some output, a cyclically-operated PDE goes through seven distinct phases of operation which, along with a general layout, is shown in Figure 5. In the first phase the filling mechanism starts the filling process. The second phase shows the PDE being filled. The time this takes is highly dependent on the filling mechanism used. In the third phase, the PDE has finished filling and the mixture is ignited. The fourth phase illustrates the detonation travelling from the closed end of the tube to the open end. The

sixth phase shows that combustion has finished. The seventh phase involves rarefaction waves aiding in the removal of the now combusted mixture [3]. It is noteworthy that the PDE need not have all of its combusted mixture removed before the filling can be restarted in a cyclic PDE.

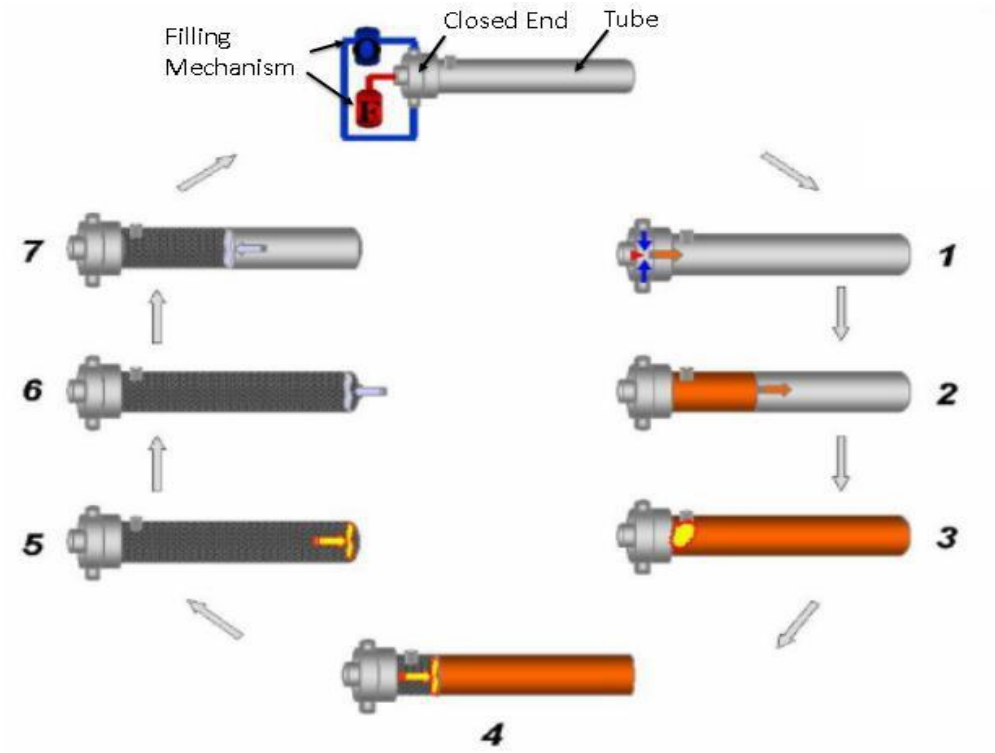

Figure 5: PDE with operating cycle. Reproduced from [3].

Chapman-Jouguet Condition

The Chapman-Jouguet (CJ) condition is a statement on how a detonation propagates during a combustion. It states that, in the reference frame of the leading shock wave, the detonation propagates at a velocity where the reacting gases reach sonic velocity as the reaction stops [5]. A later model that expounds upon that stated by the CJ condition comes from Zel'dovich, Neumann, and Doring (ZND) [5]. This model, again in the reference frame of the leading shock wave, says that the combustible mixture entering

the leading shock at a sonic velocity is compressed by it into a much higher density and hence now subsonic flow. This change causes the detonation at that area which then accelerates the flow back to the local sonic velocity [5]. It is noteworthy that combustion must stop at the sonic plane, also referred to as the CJ plane, lest there be a pressure discontinuity.

The ZND model explains detonations well and is a one dimensional model. However, detonation is fundamentally a three-dimensional occurrence with complex three-dimensional structures. Also, the apparent restriction of the flame and shock front to sonic speeds is a general approximation and in practice some portion of the flame front will be supersonic and others subsonic.

While the ZND model is both fairly simple and gives fairly accurate predictions of detonation waves, it is not ideal. Other models and solvers have been proposed that include more details and as such reflect results of experiments more closely. Since this work is primarily concerned with acquainting the reader with the overarching processes that a PDE goes through the author will not go further into the computational side.

Regardless of the model used, one of the most important parameters of the CJ condition is the velocity with which the detonation wave propagates and is given by the

term, ��. The ��equation, which is derived in other places [5, 6], is deceptively simple and is shown in Equation 3.

$$\text{��} = \sqrt{2(\gamma^2 - 1)}\text{�} \qquad \textbf{Eqn. 3}$$

In Equation 3 is the term ﷺwhich is the specific heat energy of the fuel. Similarly, the pressure associated with the CJ condition is shown in Equation 4 and given by the term ﷺ

$$\rho_{CJ} = 2(\gamma - 1)\rho_1 M^2 = \frac{\rho_1 V_{CJ}^2}{(\gamma+1)} \quad \textbf{Eqn. 4}$$

Where ρ_1 is the initial density of the mixture inside the PDE. These equations hold well so long as q is accurate. For very simple calculations of q, such as in an idealized single step chemical equilibrium equation, the V_{CJ} will be overestimated [5]. To avoid solving very complicated and difficult chemical balances by hand it is best to use already developed programs to do so. One such program is the Chemical Equilibrium with Applications (CEA) program available on NASA's website. Table 1 is a compilation of the various CJ parameters for some common fuels with pure oxygen for the oxidizer obtained by using the CEA program through NASA's website, although, it is also available for download and its source code is available. In the table M_{CJ} is the Mach number associated with the detonation wave and Φ is the mixture equivalence ratio.

Table 1: CJ states of common fuels with O_2, $\Phi = 1$, $T_0 = 300$ K, $P_0 = 1$ atm. Obtained from NASA's CEA utilizing transport properties and including ions.

	Hydrogen	Acetylene	Methane	Ethane	Propane
V_{CJ} (m/s)	2835.7	2720.1	2389.8	2116.0	2154.9
M_{CJ}	5.26	8.14	6.71	6.67	7.56
$\frac{\rho_{CJ}}{\rho_1}$	18.7	39.6	29.1	24.7	30.6
$\frac{P_{CJ}}{P_1}$	12.3	13.7	12.4	5.71	6.2
$\frac{T_{CJ}}{T_1}$	1.84	1.83	1.85	1.74	1.75

.

Detonation Requirements

There are a few basic requirements to allow detonation to be achieved and be stable. In general, the PDE itself must but be of a sufficient inner diameter and when utilizing a detonation to deflagration transition (DDT) sufficient length as well. In addition, stoichiometry also plays a role in whether detonation will occur.

Looking at a steady detonation wave, which as mentioned previously is a three dimensional phenomena, there are longitudinal and transverse shockwaves that comprise the leading shock front. These shockwaves interact and will leave a fish scale like imprint on the inner surface of the PDE as they pass. The scale like imprint is referred to as the cell and its width is referred to as its cell size (λ) and is shown in Figure 6. The cell size can be obtained experimentally from the physical measuring of the cells after a detonation wave has passed or may be calculated through mathematical models. Regardless of the manner in which cell size is obtained there is disagreement between which is appropriate [1, 8] as cell size varies between PDE's and the current mathematical models for predicting cell size show poor accuracy [8]. This is further

complicated as some fuel and oxidizer combinations, particularly methane-air, have very irregular cell sizes [9].

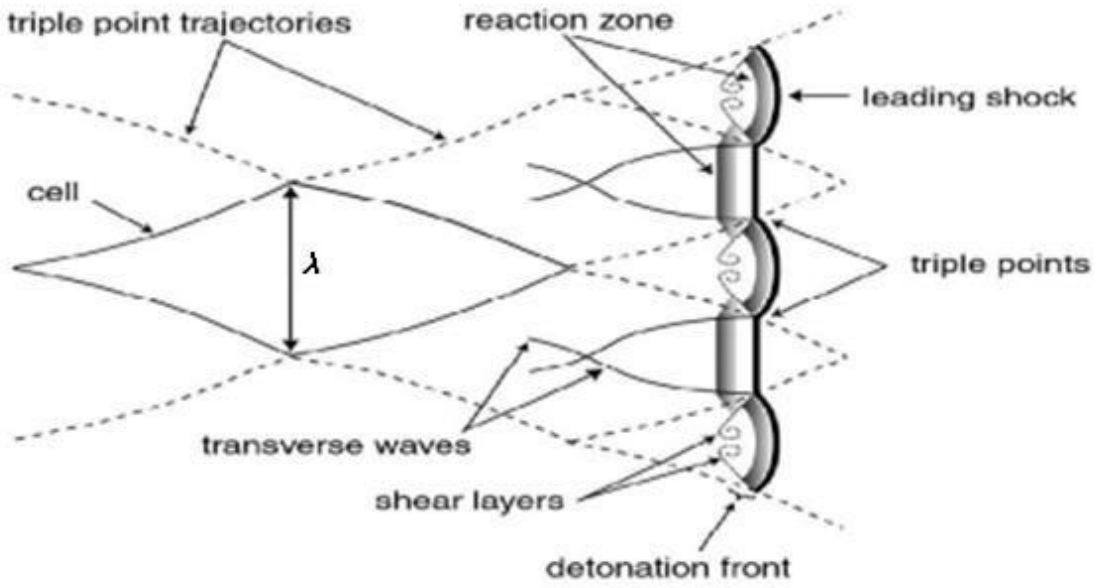

Figure 6: Shockwave and Scale pattern in detonations [8].

$$ID \geq \frac{\lambda}{\pi}$$ **Eqn. 5**

In Equation 5, ID is the inner diameter of the PDE, λ the cell size, and π is simply the ratio of circumference to diameter for a circle, or 3.14. If Equation 5 is not satisfied then a steady detonation cannot be achieved [8]. It is further noted that while detonation can be maintained with the minimum ID it will likely take longer to reach steady detonation. Table 2 shows some cell sizes from typical fuels with either air or oxygen used as the oxidizer.

Table 2: Approximate cell sizes for common mixtures. Φ = 1. Reproduced from [1, 8].

Fuel	**λ (mm)**	
	Oxygen	Air
Hydrogen (H_2)	1.3	10.9

Acetylene (C_2H_2)	0.109	5.8
Methane (CH_4)	8.0	280.0
Ethane (C_2H_6)	-	51.0
Propane (C_3H_8)	2.5	51.3
Kerosene	30.0	-

Also hotly debated is the minimum distance required for DDT to be achieved. The general consensus appears to be approximately 35λ for a detonation to be achieved but as low as 10λ [8] to as high as 1130λ [10] for a smooth walled PDE tube have been reported. However, while the minimum distance required for DDT to occur is very important there are many methods which aim to reduce this distance which allows for a smaller length of the PDE overall.

Detonation Initiation

Assuming that the requirements for detonation are met, there are two fundamentally different ways to initiate a detonation. The first method is to use some means to cause the combustible mixture to detonate and is referred to as direct initiation. However, simply causing the mixture to detonate requires a relatively large and fast deposition of energy on the order of kilojoules. This large initiation energy, as can be seen in Table 3, is reproduced from Roy, et al. [1]. In this table the lowest calculated energy requirement is for a stoichiometric mixture of ethylene and air and is equivalent to 7 grams of trinitrotoluene (TNT). This means that the required energy to directly initiate a detonation is approximately 29 kJ.

Since the large energy discharge required for direct initiation is difficult to accomplish, especially during multiple cycles, many PDE's opt for the low energy method and then try to minimize the DDT distance. By comparison, the typical energy output of a single spark event in an automobile is less than 100 mJ.

Table 3: Comparison of calculated and measured values for energy required (in kg TNT) for direct initiation of detonation for various fuel-air mixtures ($\Phi = 1$). Reproduced from [1].

Fuel in Air ($\Phi = 1$)	**Ethane**	**Ethylene**	**Propane**	**Methane**
E_{calc} (kg TNT)	0.018	0.007	0.07	120
E_{exp} (kg TNT)	0.035	0.015	0.08	10-100 (estimates)

The other way to initiate a detonation is to ignite the mixture and let it achieve detonation on its own though a detonation to deflagration transition. This can be done with minimal energy on the order of millijoules which a static discharge can provide. As with direct initiation this has issues of its own. Particularly there is some time and distance required before the mixture will achieve a steady and self-sustaining detonation.

Utilizing DDT there are distinct processes that occur from initial deflagration initiation to steady detonation. The first step is to initiate the deflagration. This is most often done by a spark which deposits a small amount of localized energy. This localized energy causes a portion of the combustible mixture to ignite and form a flame kernel. This flame kernel, as the name suggests is a small spherical flame that rapidly expands outward into the rest of the mixture [11].

In a closed cylindrical tube, such as is found in most PDE's, during expansion of the flame kernel, it forms into a hemisphere as it meets the closed end of the tube but

continues to accelerate towards the open end, as shown in the upper portion of Figure 7. The burning mixture expands causing a flow to be induced. The profile associated with this flow makes the flame shape curve even more which in turn increases the flame surface area and its acceleration exponentially [12]. This elongated flame is referred to as a finger flame which is shown in Figure 7.

The finger flame acceleration slows and stops. As its edge, known as the flame skirt, touches the wall of the PDE and due to the small angle between the wall and flame the skirt rapidly catches up to the tip of the finger flame which can be seen in Figure 7. If the skirt passes the tip then the inversion of the finger flame is sometimes referred to as a tulip flame and is characterized by the concave flame front [11] which can be seen in Figure 7. The tulip flame will then collapse due to instabilities and form a nearly planar detonation front.

Whether it is a collapsed tulip or not, the deflagration front will stop accelerating and reach a velocity that is subsonic relative to the unburnt mixture downstream of it but supersonic relative to the PDE wall. This constant velocity flow is known by several different names, (CJ deflagration, fast flame [12] or strange wave [10, 13], or choking regime [9]) and will propagate at approximately half of the CJ velocity and can potentially achieve detonation if the conditions are right. It is thought that this spontaneous detonation is formed when small hot spots form in the flow and cause pressure pulses and weak shocks to occur [14]. These weak shocks and other perturbations can culminate and form a detonation wave that can sustain itself and complete the DDT. It is noteworthy that a finger flame is not necessarily the means by

which DDT will occur and there are other mechanism such as Bychov, Combustion Instability, and others.

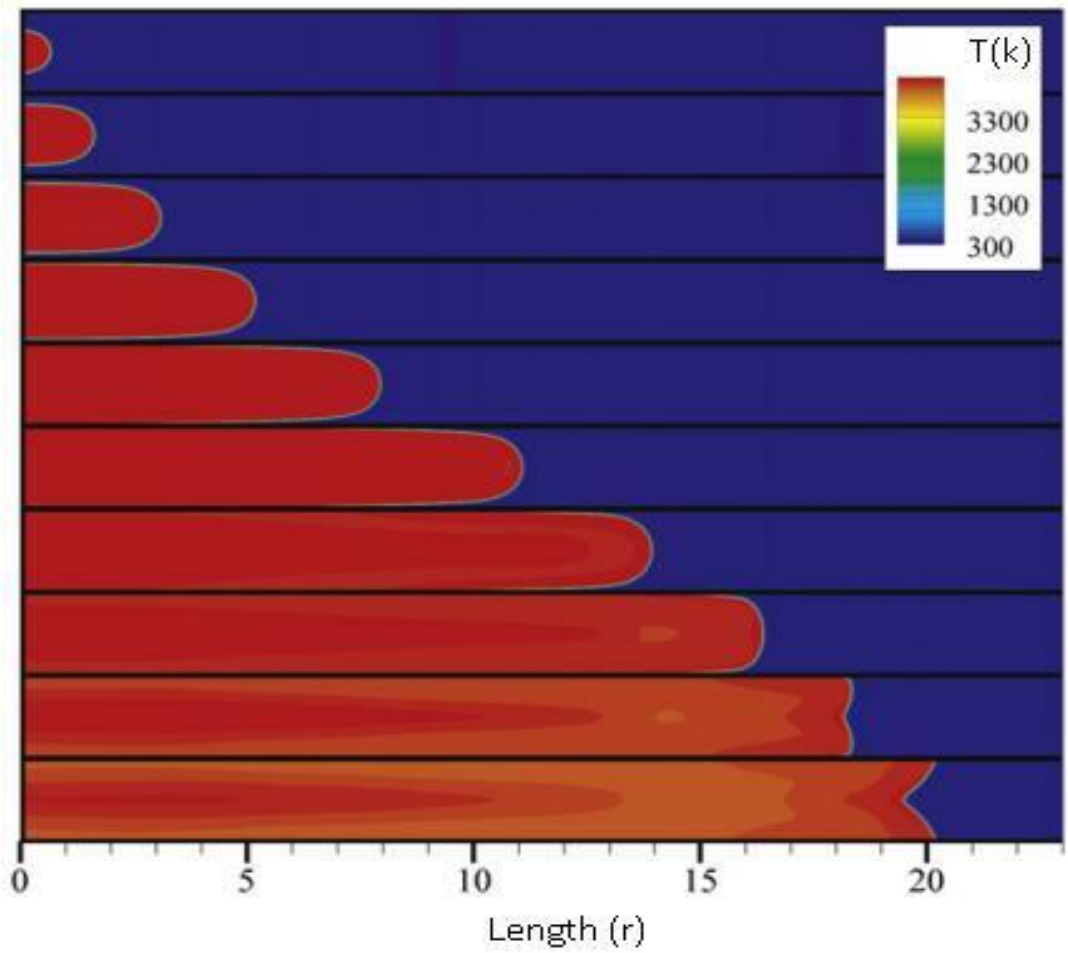

Figure 7: Tulip flame DDT from half hemisphere to flame inversion, length scale in radii of the tube [15].

Problem Statement

Based upon current research in Pulse Detonation Engines (PDE) and evaluation of current working engines, there appears to be a relative dearth of quantitative comparisons of both performance and performance enhancements against a reliable control. Furthermore, many of the current designs have a tendency of utilizing relatively expensive components and have designs that are fundamentally ill suited to alteration. It is clear that

without reliable data from a working and easily adaptable PDE that furthering the knowledge on this subject will be difficult. This work is aimed at creating such a PDE.

Objectives

The overall objective of this study was to accumulate knowledge of current working PDE's with which to compare, contrast, and ultimately build a working multi-cycle and multi-fuel capable PDE. The project was split into the following primary objectives:

1. *Investigate and evaluate current methods of tracking detonations.* The tracking method needed to have unambiguous output while, if not economical is still very robust in the face of the hostile environment that is a PDE.
2. *Investigate and evaluate current methods of multi-cycle PDE filling.* The majority of working multi-cycle PDE's either have custom valving of some sort or do not report what their mixture injection scheme is at all. In this light a thorough investigation of valves suitable for the proposed PDE needed to be performed. The hypothetical valve scheme should be simple, robust, and inexpensive.
3. *Design and fabricate a PDE.* The PDE should be capable of operating cyclically. In addition, it should be relatively inexpensive and designed with modularity and ease of adaptation in mind.
4. *Demonstration of the completed PDE.* Once the PDE was completed, its operability needed to demonstrated, and that it is capable of achieving detonation velocity, and operating in a cyclic manner with a methane and oxygen mixture.

Chapter 2: Review of Relevant Literature

In this literature review some DDT enhancements will be described along with different methods of igniting the combustible mixture. Also, two PDE's will be briefly discussed to illustrate the potential differences in design. This is done to acquaint the reader with a variety of current avenues that have been explored by other researchers and give a background for the rational for the choices which results in the PDE fabricated for this work.

DDT Enhancements

During DDT it is known that random hotspots will occur and it is thought that these hotspots are the origins of small, localized detonations that can die out or propagate until the mixture has achieved steady detonation. While the mechanism that promotes a mixture to transition from deflagration to detonation is not fully understood there are methods that are known to encourage DDT to happen in less distance. There are many methods, some are aimed at causing an increase in turbulence at the deflagrating flame front, others to coalesce the shockwaves that appear in the deflagrating flame, yet others are designed to sensitize the mixture which means to make detonations more readily achieved.

To date, there are a variety of methods that can be used to encourage turbulence in the deflagrating mixture which promotes a shorter DDT. In particular, some methods include the Shchelkin spiral, turbulizing groves, and increasing the fuel sensitivity, amongst others [16]. DDT enhancements are briefly discussed below.

Shchelkin Spiral

A method of DDT enhancement that involves blockage of the flow utilizes what is called a Shchelkin Spiral (SS). In general a SS is a blockage that is placed in the path of the flow in a PDE. It is very similar to a spring and has a blockage ratio (BR).

Wahid et al. [17] utilized a SS to assist in DDT was 50mm ID and 600 mm in length. The SS was 400 mm in length and with a reported blockage ratio of 43%. This PDE was using a stoichiometric propane and oxygen mixture with a low initiation energy estimated at 11 mJ. It was further reported that the impulse fluctuated from 30 N·s up to 98.5 N·s for its 4s run at 1 Hz frequency. The average force was 61.5 N [17] which is in line with reports from similar research. In this PDE, as in many, there is a purge phase after the detonation that clears the PDE of exhaust gases and cools it as well. This is done as a means to combat preignition which would likely ensure that detonation would not occur.

Vortex Flow

Another study, performed by Asato et al. [18] that utilized a SS that also explored the effects of vortex flow on DDT. Several SSs of differing BR, from BR = 0.36 to BR = 0.51, and lengths, 300 mm to 620 mm were used along with a variety of vortex flow velocities. The PDE has an ID of 76 mm with a length of 2220 mm. It also utilized spark ignition that was estimated between 30-50 mJ and $\Phi = 1$. It is noteworthy that simply changing from counter flow injection (where the injectors impinge on each other), to vortex flow, the DDT can be reduced between 15-43%. It is stated that when combined with a SS the total DDT reduction is between 50-57%. These numbers do seem to imply some sort of diminishing returns when multiple DDT enhancements are used together.

The authors postulate that the decrease in DDT distance from the vortex flow condition is largely from the increased initial flame velocity which, "approaches tens of meters per second depending on the rotating velocity." [1].

It is also noteworthy that one of the main issues with the SS is that it is prone to failure from the high heat. This is evidenced in reports from various institutes with operating PDE's as well as a video released showing the ejection of the PDE's SS during a firing [19]. It has been noted by some researchers [20] that if the SS is not long enough that it has a detrimental effect on DDT. Also worth reiterating is that methods which decrease DDT distance by blocking a portion of the flow sacrifice their potential thrust due to the decrease in effective outlet area.

Turbulizing Groves

A noteworthy exception to the SS which creates turbulence through blockages, is a solution which instead cuts reliefs into the wall of the PDE. In Panicker et al. [20] these reliefs are cut as a spiral grove into the wall of the PDE. In effect, this gives a SS of BR = 1. However, in the same study this was found to be less effective in reducing DDT distance than a SS. Regardless, as this encourages turbulence there is a reduction in DDT without actually decreasing the ID of the PDE which means that there is not a decrease in thrust like with a SS.

Converging-Diverging Nozzle

Another method of encouraging DDT is to use Converging-Diverging (CD) nozzle(s). The CD nozzle has a blockage ratio like the OP or SS but does not necessarily encourage turbulence and instead encourages the flow to accelerate. In Panicker et al.

[20] they note that while it does encourage DDT it is not, in their PDE, nearly as effectively as the SS utilized. Furthermore, there are durability issues such as throat erosion due to the high temperatures present in a PDE.

Fuel Sensitivity

Another way to reduce DDT is to sensitize the mixture, which can be done in a variety of ways such as including additives within the mixture. Typically, hydrogen is added to the mixture [21] but others work as well. Another additive is photosensitive nanomaterials [22]. When ignited by a xenon bulb, DDT distance is decreased by up to 50%, and also reduces DDT time.

A noteworthy exception to sensitizing the fuel is to desensitize it. This is predominately done using inert gas and is used to keep the mixture from prematurely igniting which often leads to DDT failure. This is an issue predominately present in mixtures that use pure oxygen [1].

Concluding Remarks on DDT Enhancement Techniques

Naturally, different DDT enhancements can be used in conjunction with each other. One study was performed by Huang et al. [23] which explored using two different DDT enhancements. However, there has been very little research on this and what has been done is has been in an extremely limited format. Regardless, the goal of this DDT enhancement review is not to be exhaustive but to acquaint the reader with some of the multitude of viable methods of DDT distance reduction.

Ignition Source and Energy

There are only a few methods to initiate the deflagration. The most widely used method is to use of some adaptation of an automotive system which utilizes spark plugs and typically has an output less than 150 mJ [23, 3]. However, there are a few other methods in use as well.

A novel ignition source is via corona discharge, also known as transient plasma ignition. In this method, a pseudo-spark is discharged in a timeframe on the order of tens of nanoseconds [3]. This type of ignition is characterized by many small streamers that can initiate combustion in multiple areas simultaneously. It was also found that this type of ignition source reduces the time to ignition significantly. In Rodriguez [3], it reduced the time of ignition onset by 41% and DDT by 17%. In Cooper et al. [24] it was also noted that due its unique properties, it was able to cause DDT in mixtures more highly diluted with inert gas than with a typical spark ignition. Figure 8 is a picture of a corona discharge under different conditions [25] all of which off improvements in both DDT distance and time as compared to traditional spark ignition source.

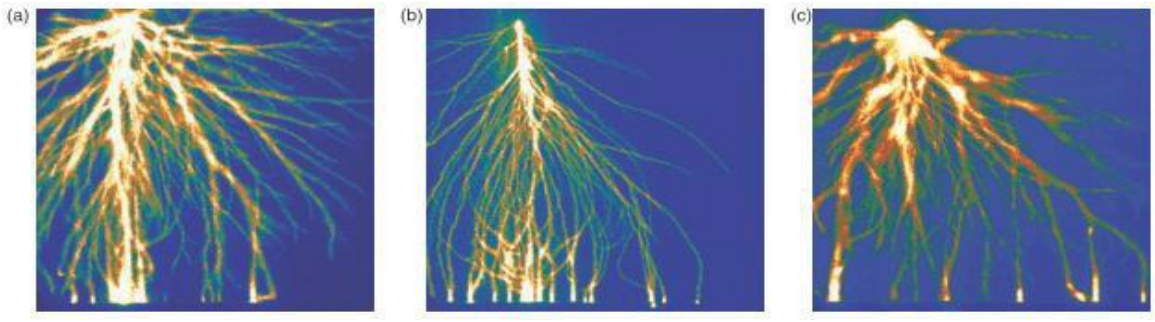

Figure 8: Photo of Corona Discharge in Air at 25 kV. (a) is the basic circuit, (b) with a 23 kΩ series resistor, (c) with a 10 μH series inductance [25].

This brief overview of different ignition methods was to introduce the idea that different methods can result in different DDT outcomes.

Current PDE's

One PDE from Ke et al. [12] was designed to be used with liquid kerosene and oxygen for the detonable mixture and utilized a mechanism rotary valve to inject the mixture. The choice of liquid kerosene means that this PD is operating with a mixture of two-phases. One phase being liquid and the other gaseous presents unique problems covered in the article on this PDE. In addition, the PDE uses a SS as a DDT enhancement, an automotive spark plug for ignition, and pressure transducers to track the detonation. A schematic of the device can be seen in Figure 9.

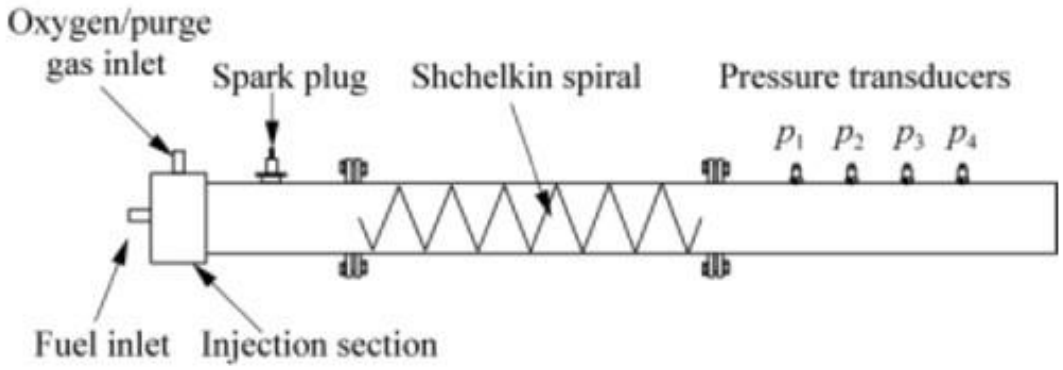

Figure 9: Design overview of PDE used by Ke et al. [12].

Part of the rotary valve setup is illustrated in Figure 10. This method of filling is robust but also has a constant leakage of mixture into the PDE due to its design [12]. Also due to the rotary valve there is an almost negligible leakage of detonable mixture to the atmosphere as well.

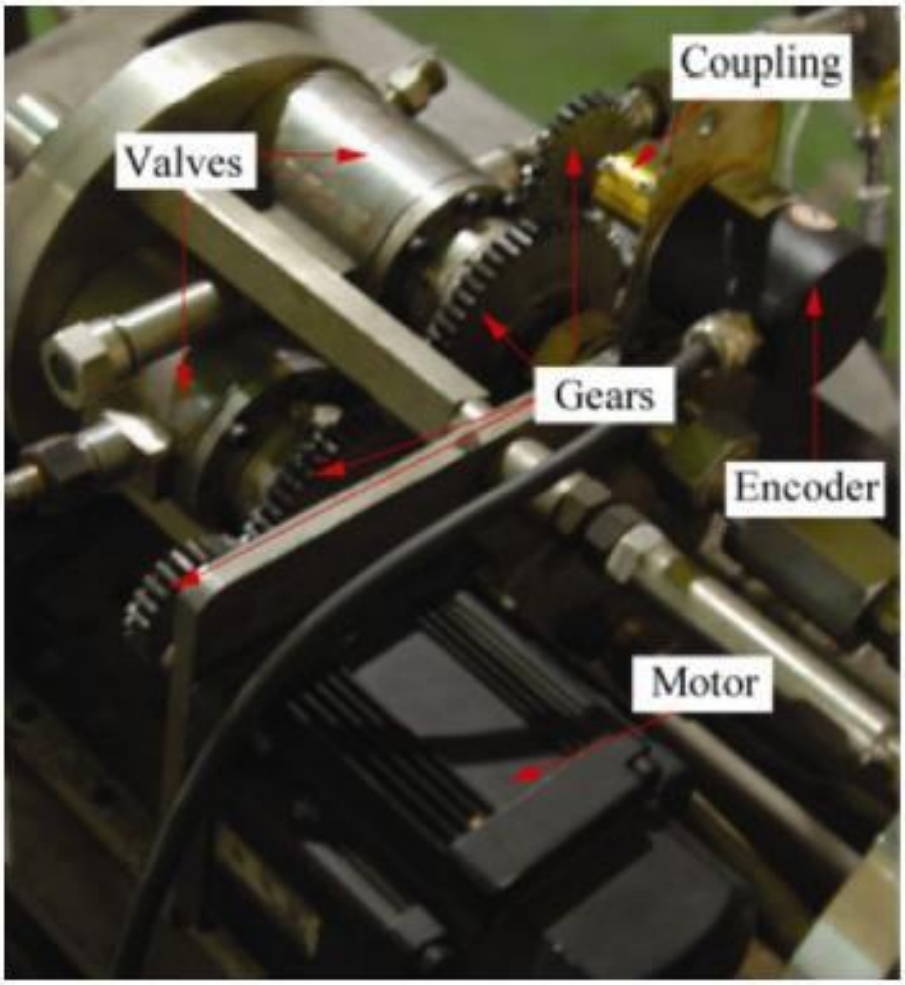

Figure 10: Rotary valve used by Ke et al. [12] in PDE.

Another PDE was a demonstration model designed and built as West Virginia University (WVU) for testing detonations in a miniature PDE [26]. The PDE, shown in Figure 11, was used to explore the feasibility of utilizing miniature PDE's in disposable unmanned aerial systems. It monitored detonation using capacitive discharge microphones and was able to achieve detonation with a SS DDT enhancement. Unfortunately, due to this PDE's small size, it is unable to achieve a steady detonation with a wide range of detonable mixtures [26]. It is also unable to operate cyclically. These two shortcomings were the primary reasons that the new WVU test bed PDE was conceived.

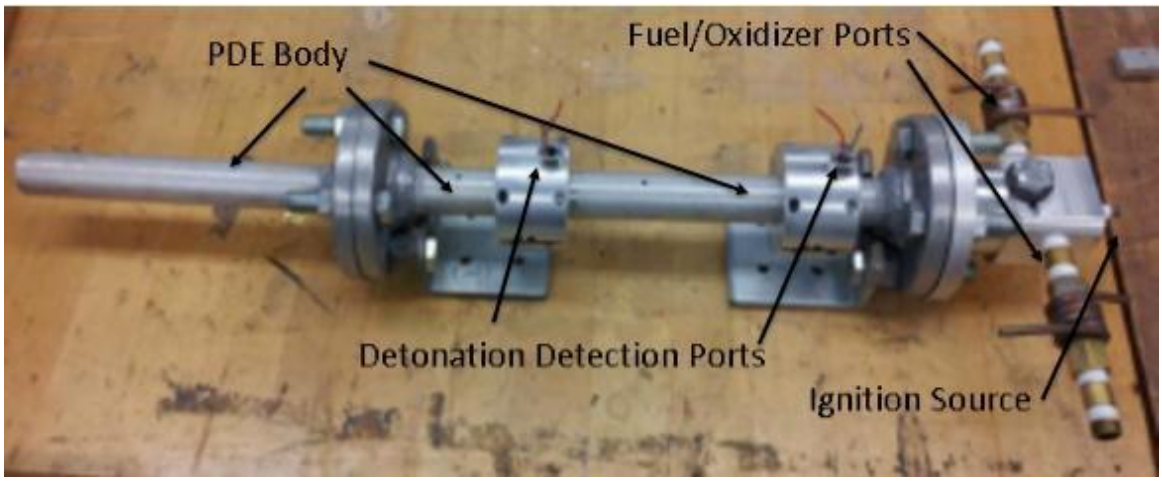

Figure 11: WVU miniature demonstrator PDE [26].

Chapter 3: Evaluation and Selection of PDE Parameters

Design Overview

The goal of this research is to design, fabricate, and test a PDE test bed that could be utilized for a wide range of future research. A list of design requirements was made along with their relative importance. The four requirements that vied for top priority are:

- The first is that the finished PDE must allow for a multitude of fuels and oxidizers. While only one mixture would be used in the initial data collection tests limiting the possible mixtures would limit the PDE's use as a test bed.
- The second was that the PDE must be able to be run for multiple cycles.
- The third was that the design must be modular and allow for easy modification. Designing for modularity allows for future modules to be more easily added in the future.
- The final criteria was that the PDE be inexpensive. If cost of the PDE and its constituent parts is not kept in mind during the design then budgeting could become an issue during its fabrication or when future modules are implemented.

Each of these main priorities has a strong influence on the final design. If the PDE were to be designed to run as many different fuels and oxidizers as possible then the possibility of it being inexpensive, both in building and operation, could not be accomplished. Likewise, aiming for a high operational frequency in a valved design would necessitate many expensive valves and the appropriate controllers for them. Fortunately, if the modularity was incorporated into the design properly it would require little extra initial cost and greatly reduce the cost of future modules. Since inexpensiveness was a concern the PDE was designed with initial and potential future costs kept firmly in mind.

As with most engineering challenges many of the systems are designed simultaneously. Both the choice of material and general design of the PDE are intrinsically linked. However, with a very general and basic design these choices can be separated. A very basic design in terms of a PDE is a tube of constant diameter and sealed at one end where the ignition device(s) and feed(s) for fuel and oxidizer reside. This design was chosen largely to have a very general and non-specialized starting point for future modules as well as to allow comparability to most other PDE's in existence.

Main Body

Referring back to the cell sizes in Table 2 it can be seen that most fuel and oxidizer mixtures can achieve and maintain detonation at PDE inner diameters of two inches and under. Coincidentally, this ID is also where the cost of tubing increases dramatically. Because of this, 4130 steel tubing with an ID of 2.01 inches was chosen for both its mechanical properties and its cost.

With the general design settled, a way to make the design modular was investigated. As different experiments have different requirements ranging from sensing mechanisms, viewports, or other devices to include their placement it is conceivable that over time the PDE itself could be altered drastically as new ports are added and then later plugged. Due to the general design requirements of the PDE it was thought that sections could be made that would be removable. Each removable section could be altered as needed. Furthermore, removable sections can be moved around or exchanged for others as needed.

Since a PDE has such large pressures, if the tubing is partitioned sealing becomes an issue. To allow these sections to be made, several sealing options were explored. The initial idea was to treat the tube like any other pipe system and purchase appropriately rated industrial joints. While this would be perfectly acceptable and sufficient even the simplest of these joints are very costly. It was also seen from other PDE's that utilized these joints that sealing could also become an issue [19] as the majority of these joints are simple flat interfaces pressed together via a force perpendicular to the mating surface.

Labyrinth seals were also investigated. These could be created by machining the sections of the tubing to within very tight tolerances where they joined. The labyrinth seal works by extending the distance the escaping fluid would have to travel to escape and lowering the likelihood, or amount, that escapes via either sealing or pressure drop respectively.

Since the tubing is not a single piece it will need to be held together against axial forces as well. To do so, an inexpensive solution was sought and found in the form of automotive V-Band clamps. These clamps have a half-V section with a flat face that

mates to another of the opposite orientation and as welded to either end of the tube section. The clamp then mounts over them and utilizes pressure to hold them together: as hoop tension in the clamp is increased, the compression between the faces of the joint is also increased. These clamps also add both safety and extra labyrinth sealing to each joint.

In addition, each section of the PDE has a foot welded to it with holes such that it can be directly bolted to a table. The foot on each section also allows the PDE to be attached to other things such as a system that would only allow a single degree of freedom for force measurements. With the culmination of these different solutions and design points, a PDE that has a barrel which is safe, cost effective, and modular has resulted.

Figure 12 shows two of the fabricated sections. In particular the V-band half sections and the labyrinth can be seen by following the path escaping gasses would have to follow to reach the atmosphere. Figure 13 shows the previous two sections clamped together.

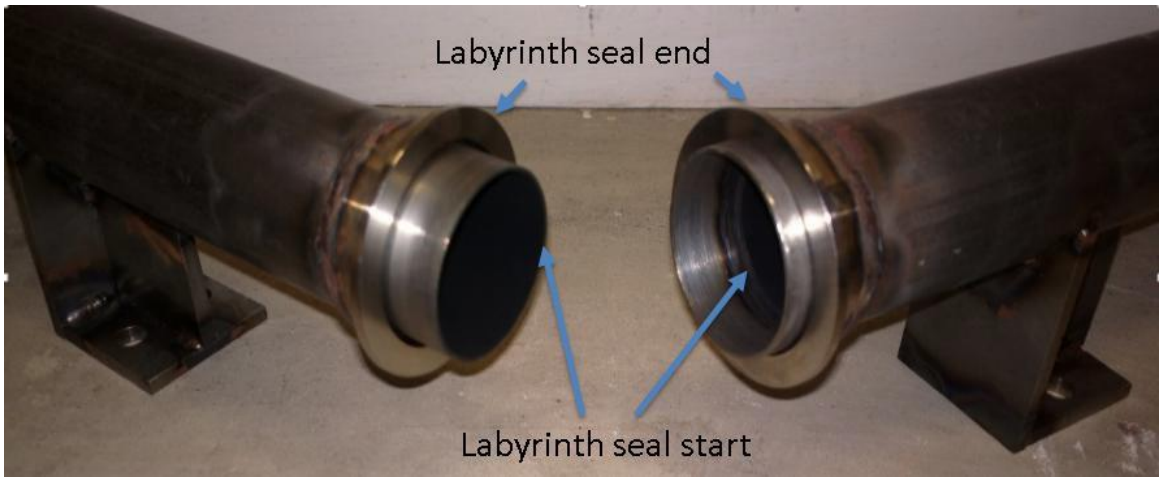

Figure 12: Picture of PDE sections showing labyrinth and V-band sections. Labyrinth seal follows machined ends and V-Band.

Figure 13: Previous two sections joined and clamped together.

Head and Ignition

One of the primary benefits of having a system designed to be modular from the very beginning is that altering system parameters can be done much easier than otherwise by changing a module. Another notable benefit of this is that multiple head designs can be fabricated for the PDE and quickly interchanged. In keeping with the design parameters and that the PDE would need a baseline to compare later alterations to for performance enhancement comparisons, a simple design was chosen. This design would not use any known enhancements that can be incorporated into the head. It would simply have a port for fuel and oxidizer coming in along the same axis directly opposing each other but impinging upon the ignition source. The ignition source is located on the closed end of the PDE along the central axis that runs the length of the PDE. This can be seen in Figure 14.

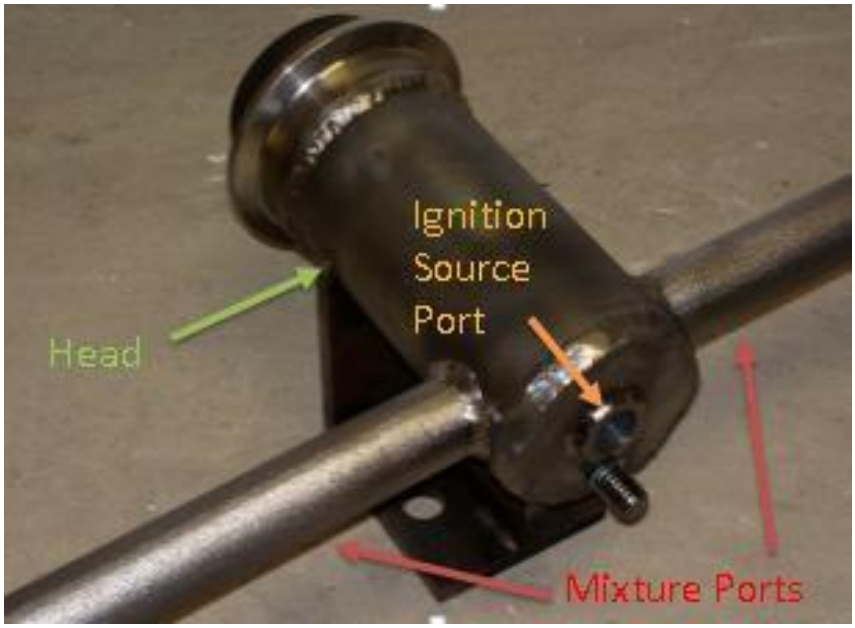

Figure 14: Picture of completed standard PDE head section.

Much like the head design the ignition source was chosen to allow an accurate baseline for later comparison. It was also chosen to be simple and robust. An automotive system was chosen for these reasons. It was also chosen because the signal required to initiate a spark is similar to the one that controls the fuel and oxidizer.

Valving and Fuel Injector

The PDE, as with any engine, must be able to get sufficient fuel and oxidizer to run at the desired operation parameters. For a PDE with an internal volume of ~0.9 gallons (~3.4 Liters) the requirements for fuel and oxidizer increase linearly with increased volume or increased operating frequency. For instance, if the PDE is to be run at a frequency of 10 Hz it would require, at a minimum, a volumetric flow of ~9 gallons of fuel and oxidizer a second. While a steady flow of this magnitude is not necessarily difficult to achieve it becomes difficult when the flow is often intermittent because of the valves.

To achieve this type of flow some form of valve that is able to flow large quantities of the various fuels and oxidizers at the desired frequency in a safe and controlled manner is required. In general, the issue of safety limits this type of valve to one with a sealed body that has no leakage. As rotary valves are notorious for their leakage to the surrounding environment as they wear as well as generally being difficult to setup they were quickly abandoned as a valve candidate. In general, the only valve type that meets the requirements is some form of plunger valve. These valves come in a variety of sizes and flow rates and with varying control requirements. They have the added benefit that when the valve mechanism wears, if it starts to leak, it leaks along the path that the flow travels as opposed to into the environment. Figure 15, shows a typical automotive fuel injector which is a form of a plunger valve.

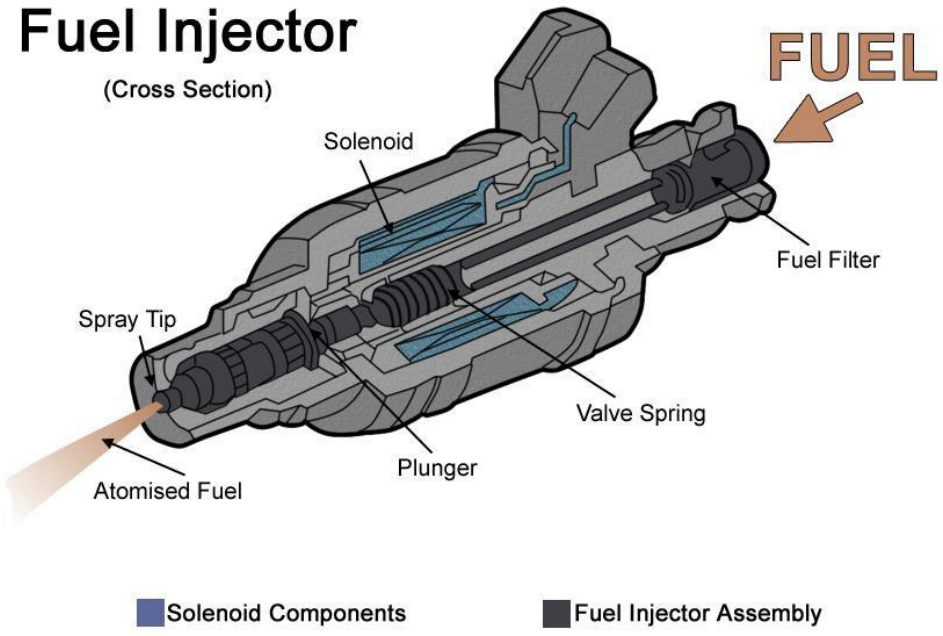

Figure 15: Typical fuel injector cutaway. Reproduced under GNU Free Documentation License.

After an extensive search through different manufacturer's valve catalogs only three candidates were discovered at the time. Every other valve that was found either

flowed enough for 10 Hz operating frequency if enough valves were present but were unable to be actuated fast enough or could be actuated quickly but the required number of valves made it cost prohibitive. Accurate comparisons were essential to ensure a cost effective system was chosen.

Table 4 is based upon theoretical calculations where the information is available. It should be noted that despite contacting the USA representative and distributor for Matrix valves no extra information was given besides the listed flow rate. As such, the listed flow rate was used across the board and this most likely overestimates the 891's capabilities to some extent. It is also noteworthy that each valve requires a different control scheme. The MechTronic valve is an automotive valve and its control scheme can be accomplished with relatively inexpensive off the shelf automotive parts. The 891 is similar to the MechTronic valve in this regard but is designed for industrial and scientific applications and with a much more expensive off the shelf controller. On the other hand the H2100 is an automotive valve but would require a custom controller to be designed, tested, and built.

Since all of the valves operate in a choked flow regime the effective orifice size was back calculated using the Equation 6 and then the steady state mass flow was calculated for a single gas and then the comparison made in Table 4. In Equation 6 the $\dot{m}$ term is the mass flow rate, the A^* term is the sonic throat area of the valve which is the minimum area present in the valve and where the flow through it becomes sonic. The R term is the specific gas constant and the γ term is the ratio of specific heats for the particular fuel or oxidizer being used. The T_0 and P_0 terms are the total pressure and temperature respectively of the gas that will pass through the valve.

$$\dot{m} = \frac{A^*}{\sqrt{R_{gas}}}\sqrt{\gamma\left(\frac{2}{\gamma+1}\right)^{\left(\frac{\gamma+1}{\gamma-1}\right)}} \quad \textbf{Eqn. 6}$$

Since all three injectors have different maximum pressure ratings and the PDE is designed with different fuels and oxidizers in mind the A^* will be what is primarily reported later in this work as it is both easier to generalize expected flow with and because for the chosen valve it needed to be experimentally obtained.

Table 4: Comparison between different injectors.

	H2100	MechTronic	891
A^* (mm^2)	4.04	1.76	24.23
$\dot{m}$ (g/s CH_4)	5.6	2.1	31.6
Cost per Injector ($)	76	130	241
Controller cost per Injector ($)	~15	~19	300
Required Injectors (10 Hz)	21	55	4
Estimated Total Cost ($)	1911	8195	2164

Comparing the three valves, the MechTronic valve simply fails to live up to the others in the price per flow category and would require much more plumbing due to the large number of valves that would be required. Naturally, more plumbing necessitates more cost and time spent building said plumbing. However, the MechTronic valve is an automotive type valve that is easy to acquire and comes with responsive support from the manufacturer in the USA. Also, the means to control the MechTronic valve are both inexpensive and plentiful in the form of standardized controllers also meant for the automotive industry.

The Matrix 891 valve is very appealing in that it would require very little plumbing and when considering just the valve, relatively inexpensive from a cost vs flow perspective. Unfortunately, as each 891 valve requires a controller that costs nearly as much as the valve itself its overall cost per performance drops dramatically. Also of note was a general difficulty in getting data on the 891 from the representative which brings in large questions about what future support might be available. Despite these issues, the 891 would be a predominately all-inclusive plug-and-play system and need minimal customization.

The HANA H2100 appears to be a very good compromise between the MechTronic and Matrix valves. The H2100 would require much less plumbing than the MechTronic with those associated benefits while maintaining a cost vs flow similar to the 891. However, the H2100 has no USA support and no controller that could be utilized for the PDE application. An electrical engineer that specialized in motors and controls was consulted and it was explained that the controller for the H2100 would not necessarily be difficult to create and that it would also be relatively inexpensive to do so.

After the pros and cons of each valve were evaluated, it was decided that the H2100 would be tentatively selected and one was purchased for testing. The deciding factor was that while both the H2100 and 891 had poor support the H2100 was relatively inexpensive per unit. This meant that if some failed they would not be as expensive to replace as the 891. Also in the event of failure, the PDE could run with a few failed H2100's but would likely be unable to operate at all with only a single failed 891. Furthermore, in light of the poor support, it was still known that the H2100 is a standard solenoid actuated valve while the 891's operation was entirely unknown.

Valve Control

Now that the injectors were chosen and they did not have a controller one needed to be designed and built. A simple method using basic 555 timers to output the pulse width modulation (PWM) required by the valves was chosen after speaking with an electrical engineer. In addition, a program was used that could accurately model the circuit before any components were purchased, assembled, and tested. While there are methods other than a hardware controller that can output the required PWM to control the valve this method was chosen because it would only require power and a continuous input signal for the on time desired for the valves. A continuous input is typically easier to program and output in various program suites and data acquisition units (DAQ). This simplification reduces programming time for the current DAQ and any future ones. The PWM circuit is replicated in Figure 16.

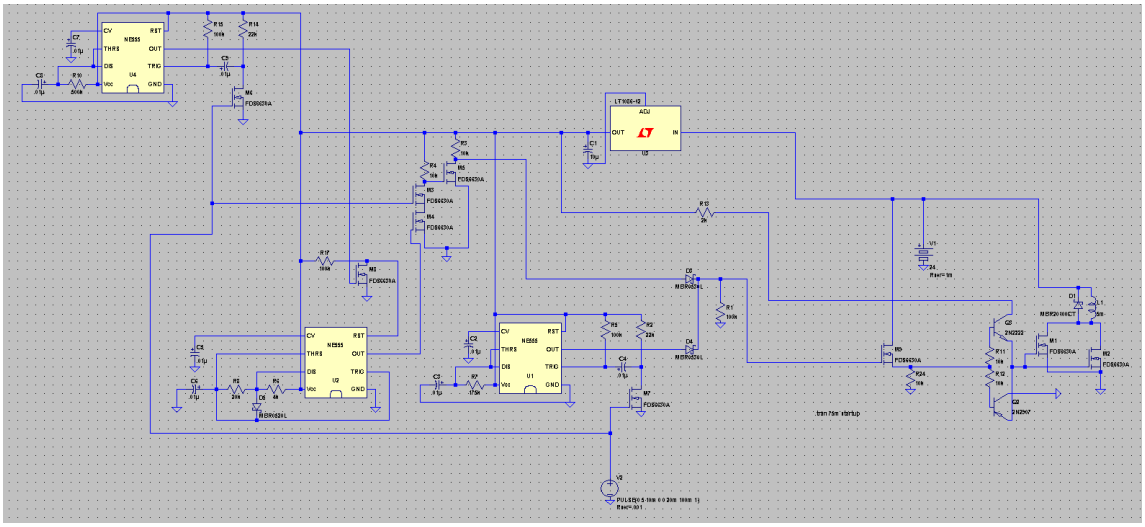

Figure 16: Complete PWM circuit.

The circuit utilizes three 555 timers. The following is a very simple explanation of the use of each timer. One of the timers is used in monostable mode for the initial peak in

current needed to quickly open the valve. Another timer is used in astable mode to actually PWM the power on the valve to hold it open but not overheat or otherwise damage it. The final timer is used in monostable mode to delay the onset of the PWM after the initial current peak to allow the current in the peak to drop off. Together they work to deliver a peak, delay the onset of PWM for the current to drop to hold levels, then PWM until the signal that started the process was removed. Also, due to differences between any two electronic components the circuit was designed with rheostats that could be used to tune the circuit to have the desired output. Furthermore, since two of these control circuits would be needed, one for the fuel and one for the oxidizer, the rheostats would allow the controllers to be matched.

The three 555 timers made up the control side of the circuit that actuated the valves. The power side of the circuit, in essence, took the peak and hold output of the control side and switched on and off in time with this output. However, this could not be done with a standard relay as the on and off switching must be done much faster than even solid state relays are capable. As advised, transistors were looked into and a relatively simple circuit using them as switches was designed which could switch in time with the control signal.

After building and testing the PWM circuit with an oscilloscope and later a valve itself the circuit was found to work as desired and the rest of the parts needed to control and switch the 21 valves was ordered. Also at this time yet another program was used to design a circuit board for all of these components. This was done to ensure the circuits could not be altered with a casual bump as can happen with breadboards. It also greatly reduces the wires being run around the PDE which can only be considered a good thing.

The circuit board design was then sent to a fabricator that specializes in small run boards to be manufactured. The assembled board can be seen in Figure.

Figure 17: Assembled PWM circuit board during QC testing.

Since the control circuits would need to be tuned after assembly and would be tuned based upon the current running through the coil several options were investigated to do just that. A current probe for an oscilloscope would have been ideal, however, they can be very expensive. Another solution would be to use an on board current sensor originally designed for boards to monitor the current of some other part of the circuit. Given that this would be a much cheaper way to do the exact same thing a simple board was designed and sent to a fabricator. The assembled circuit allowed the current through the coil to be monitored and the control circuits tuned to the valves specifications of 7A peak and 2.5A hold currents.

Valve Manifold

The valves need something to both hold them in place and contain a reservoir of either the fuel or oxidizer. The reservoir also needs to be large enough such that there will not be too large of a pressure drop before the pressure regulator reacts. It was determined that a reservoir that contained twice the required amount of fuel or oxidizer for a single shot would be sufficient. It also needs to be able to converge the flow of multiple valves and not impede their flow. In addition a fast reacting one way check valve was added just after the flow convergence. This, along with keeping the fuel and oxidizer segregated until both have entered the PDE head, increases the safety of the device as a whole. A rendering of the manifold can be seen in Figure 18.

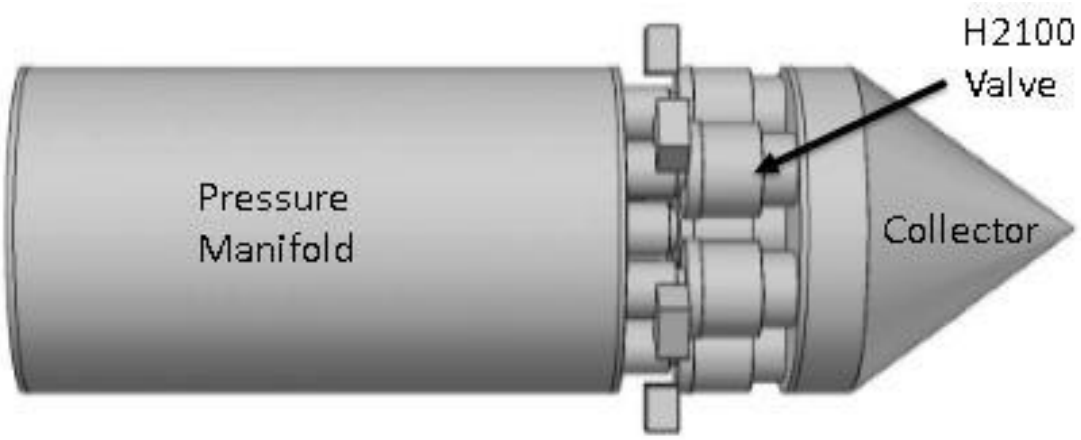

Figure 18: CAD rendering of PDE manifold.

After the initial valve testing it was seen that most of the fuels that the PDE could reliably use would require one third of the 21 injectors and two thirds for the oxidizer when oxygen was used. This works out rather well as it allows a simple configuration of the manifolds, specifically, a hexagon orientation with the seventh injector in its center. This allows three identical manifolds to be made which simplifies manufacture as well as testing. An assembled and ready to use manifold is shown in Figure 19.

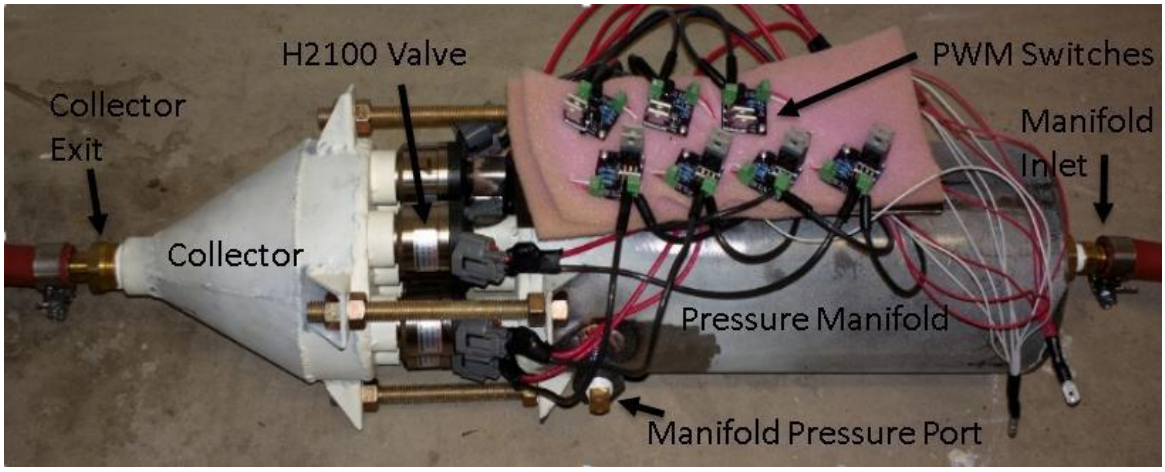

Figure 19: Assembled manifold with plugged pressure port and PWM switches in place.

Once the manifolds were made ports were added to each in the same place that would allow the pressure inside to be monitored. After the manifolds were made, both the reservoir and converging nozzle were pressure tested to 100 psig in a hydro test to ensure they did not leak. Several leaks were found and sealed. Once the manifolds were leak free they were then pressure tested to 140 psig which is beyond what would be seen during any tests.

Ionization Probes

Much like the valves and their controllers there are methods that are established but that tend to be either convoluted or expensive. Not only this, but most means to detect the passage of a detonation wave are also temperature sensitive. This includes dynamic pressure transducers and microphones alike. Even some off the shelf ionization probes that detect the ionized gases behind the detonation wave can potentially melt in the high temperatures possible in a PDE. There were schemes to increase the longevity of all of these methods but in most chases required some form of active cooling or simply buying cheap sensors and replacing them as they were destroyed in the case of the microphones.

Upon evaluating these options it was found that a simple ionization detection probe could be made from an automotive spark plug. This would allow for both an extremely robust probe that would be able to detect the passage of a detonation wave as well as very inexpensive solution to a normally very costly problem. Ionization probes utilizing a Wheatstone bridge circuit where tested using the WVU miniature PDE. This probe was found to effectively and reliably detect the passage of a detonation wave.

However, the primary downside of this is that the probe sticks into the flow and as such will have some effect on it. Despite this and keeping in mind the objectives of this PDE it was judged that the pros outweighed the cons. A circuit board was designed to simplify and allow clean, quick, and easy installation or removal of the probes. The circuit was different in this iteration such that upon detecting the ions it would show a voltage rise and a sharp peak as opposed to a voltage drop into a steep valley that the Wheatstone bridge circuit gave as an output.

Chapter 4: Testing

Several tests needed to be performed before the PDE could be operated. One HANA H2100 was purchased and first needed to be tested to verify that its performance is similar to that found in the company's literature. These initial tests would be mass flow tests to back calculate the valves A^* value. The valve would be tested at its listed maximum pressure value to ensure it can reliably do so.

Following a successful valve test more valves were ordered and manifolds fabricated to hold the valves. The valves were then tested in the manifolds and the

effective A^* of the entire assembly was found through testing. These values were in turn used to setup the PDE's equivalence ratio.

With the PDE setup it will then be initially operated to ensure that detonation is occurring. After detonation is verified the PDE will be operated cyclically and detonation verified at frequency with the IPs at different locations.

Valve Testing

Initial Valve Testing

In the manufacturer's literature it is stated that the H2100, like many automotive solenoid valves used to control fuel, requires a peak-and-hold type controller (also called pick-and-hold) to realize its best performance. Peak-and-hold control works by initially allowing a current to pass through the coil until it hits a peak value and is then lowered to the hold current value until power is removed. The initial peak current is used to quickly open the valve and is especially useful at pressure ratings near its maximum value. Due to the H2100 being designed for diesel systems and that it operates at both a higher voltage and current than its gasoline counterparts it cannot utilize the single chip solutions that they do. Since a control system was not available that could handle this the H2100 was instead initially run and tested in a saturated mode. Saturated mode does not have the initial peak in current that peak-and-hold mode does and instead simply supplies the hold current from the beginning. This would undermine the H2100's performance since it could take upwards of ten times longer for the valve to open, if it does at all at higher pressure settings, as advised by an electrical engineer.

Due to the aforementioned limitations the initial injector testing was simply to see if it could reliably open at a variety of pressures using a simple saturated circuit which

can be seen in Figure 20. Appropriate components were purchased and the circuit was built and tested and found to reliably open the valve at pressures above its rating.

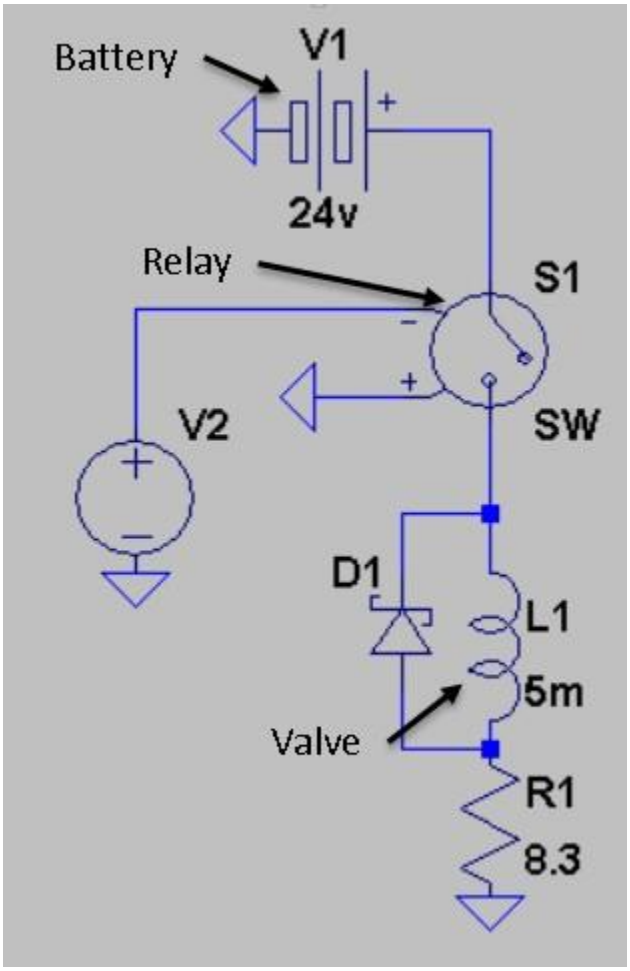

Figure 20: Saturated circuit diagram.

Also at this, time a simple controller was designed using a LabJack and LabView. This would control the relay which in turn controlled the power to the valve. However, given that this control scheme was far from ideal the valve would need to be characterized to ensure that for a given input command the valves open time was known. This was accomplished by pressurizing the valves input and having its output impinge on a pressure transducer as shown in Figure 21. There was a vent along the output to ensure that the pressure transducer was not overpressured.

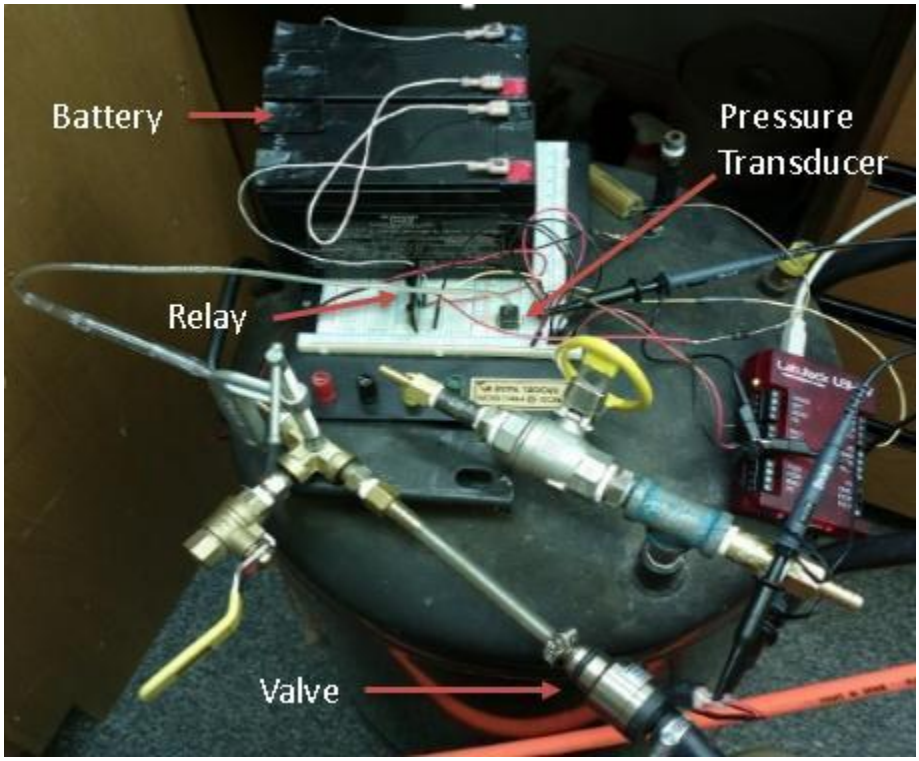

Figure 21: Injector timing testing setup.

The valve was tested at a variety of different pressures and commanded time durations and the resulting flow time, that is the time of the output of the downstream pressure transducer, was recorded. The timing, both the commanded on time and the output of the pressure transducer were captured with an oscilloscope as can been seen in Figure 22.

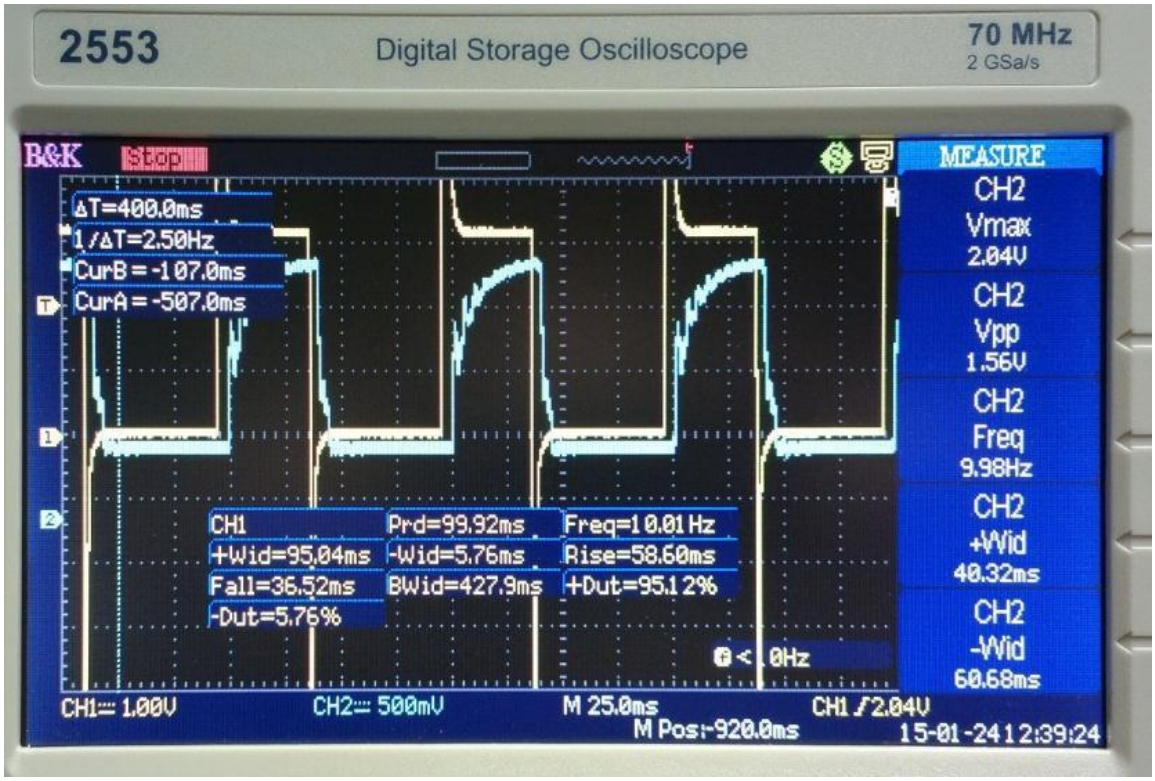

Figure 22: Commanded on time (yellow) with pressure transducer output (blue).

With a mapping of how the valve reacted with that particular circuit valve testing was performed and it was found that the H2100 performed similarly to the published values.

Manifold Testing

With the manifolds designed and pressure tested it was time to test them and characterize their flow properties. This characterization was required to be able to effectively and accurately calculate things such as fill percentage and stoichiometry.

The characterization of the manifold was performed as follows. The finalized manifold system was utilized, that is to say using all the associated circuitry, controllers, and programing that will control the PDE. The system was setup as directed in Appendix C. The system was pressurized with air that flowed through a valve. Once the system was

pressurized the valve was closed to ensure that no more air could enter. The valves were then opened for a specified amount of time and the pressure history recorded with a calibrated pressure transducer. This pressure history could then be used to calculate the effective A^*, or effective sonic throat area, of the entire system. More details on the calculations as well as some of the data and results are available in Appendix D. Figure 23 shows the general setup utilized to perform these tests.

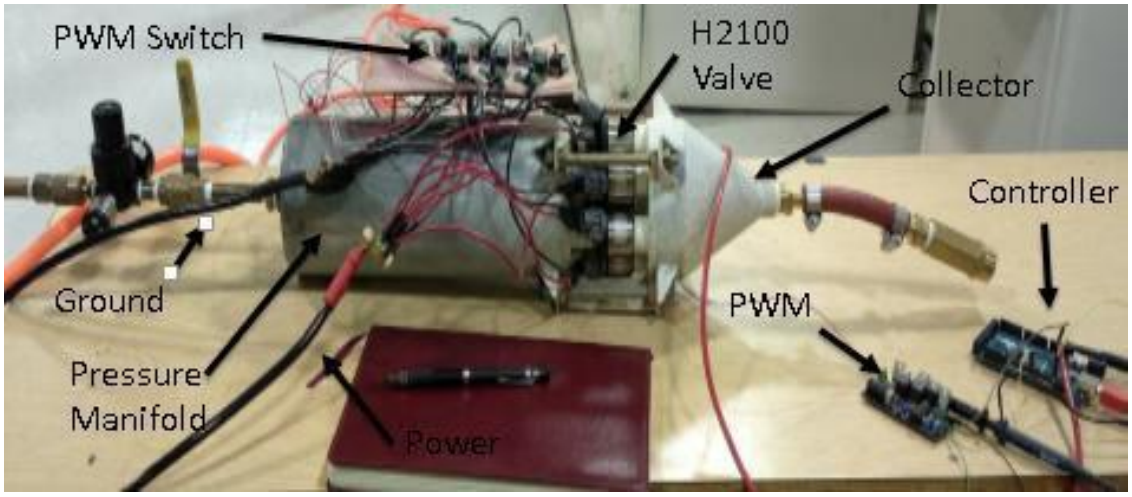

Figure 23: Manifold testing setup.

PDE Testing

For testing, the PDE was setup as shown in Figure 24 and Figure 25. In general, the manifolds were connected to their respective pressure regulator and the pressures set such that an $\Phi = 1.00$ was expected. The various sensors were connected to power and the DAQ. The controller was connected to the PWM circuitry. Finally, the PDE head was connected to the manifolds and the ignition source attached. All grounds were connected to ensure there would not be any DC offset. More details on the PDE setup can be found in Appendix C.

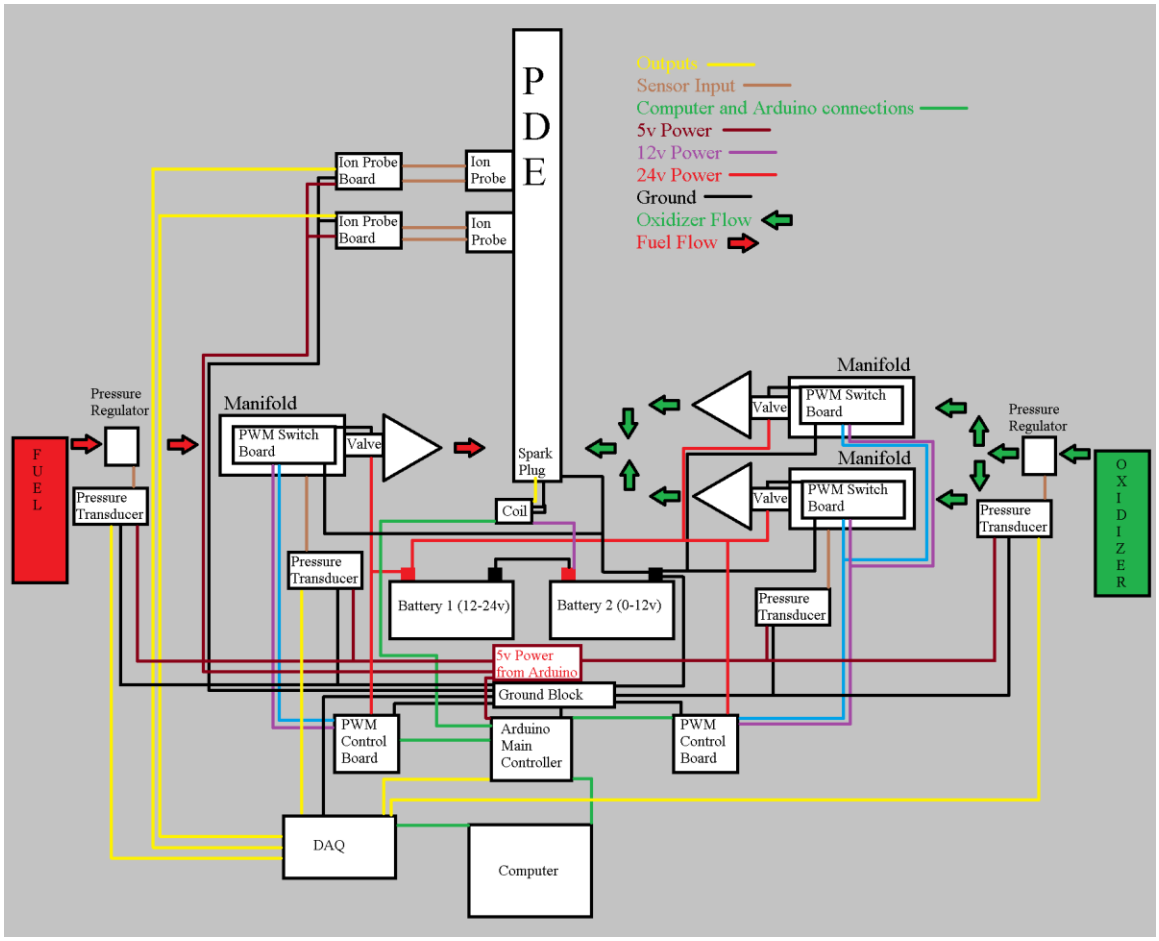

Figure 24: PDE setup diagram.

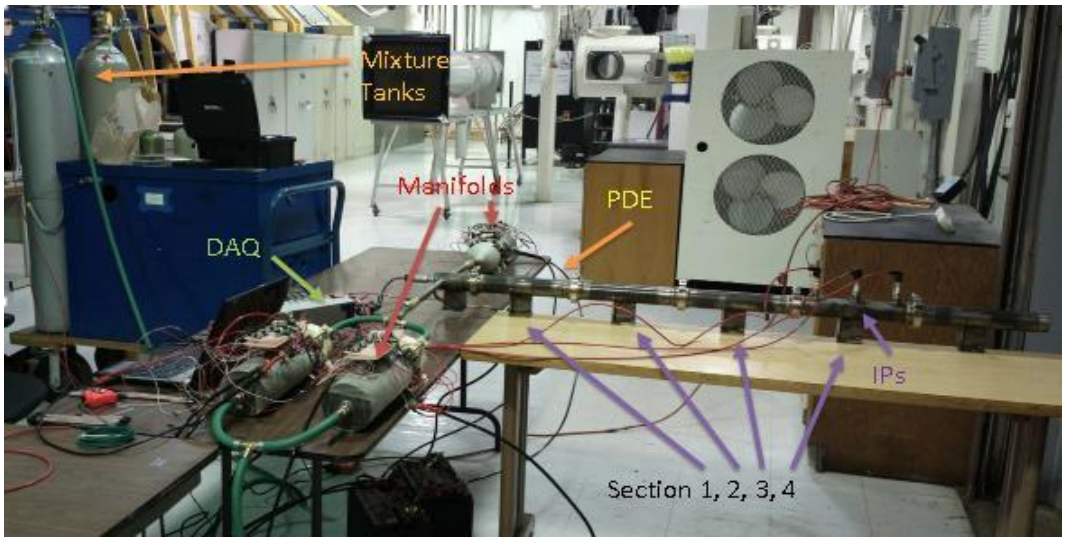

Figure 25: PDE setup with IP.

For detonation verification the section that contained the ion probes was placed as far from the head as possible, in section 4. This was done such that the IPs would be able to detect a detonation in the case of a long DDT. This can be seen in Figure 25 which shows the general layout of the PDE when setup. As can be seen, the PDE was placed in such a manner that the end of it is slightly outside of the building and furthermore that there is nothing in front of it.

The test matrix can be seen in Table 5. The PDE was run initially in single shot mode, that is to say not cyclically, to verify detonation. The PDE was fired once and data collected then allowed to cool this was repeated 16 more times. The IP section was then moved to position 3 and cyclic testing commenced. Cyclic testing was done by firing the PDE at a specified frequency while collecting data. Once the IP section was moved to position 1 the 1.5 Hz cyclic operation frequency was verified to show detonation. After this, the PDE was operated at much greater frequency 10 Hz and 20 Hz respectively and data collected.

Table 5: PDE test matrix.

IP Section Position	*Fuel*	*Oxidizer*	*Φ*	*f (Hz)*
1	CH_4	O_2	1.00	1.5, 10, 20
2	CH_4	O_2	1.00	0.25, 0.5, 1, 1.25, 1.5
3	CH_4	O_2	1.00	0.25, 0.5, 1, 1.25, 1.5
4	CH_4	O_2	1.00	N/A

Chapter 5: Results

Manifold *A** Testing

The finalized valve manifolds were tested to find their respective *A** values. To reiterate, the *A** was the value that needed to be tested and is the value in the mass flow equation that cannot be easily changed. In Figure 26 the calculated *A** is shown for each test run can be seen along with the calculated error for the fuel manifold. The average of these values is taken as the true value and has a value of 25.96 mm^2.

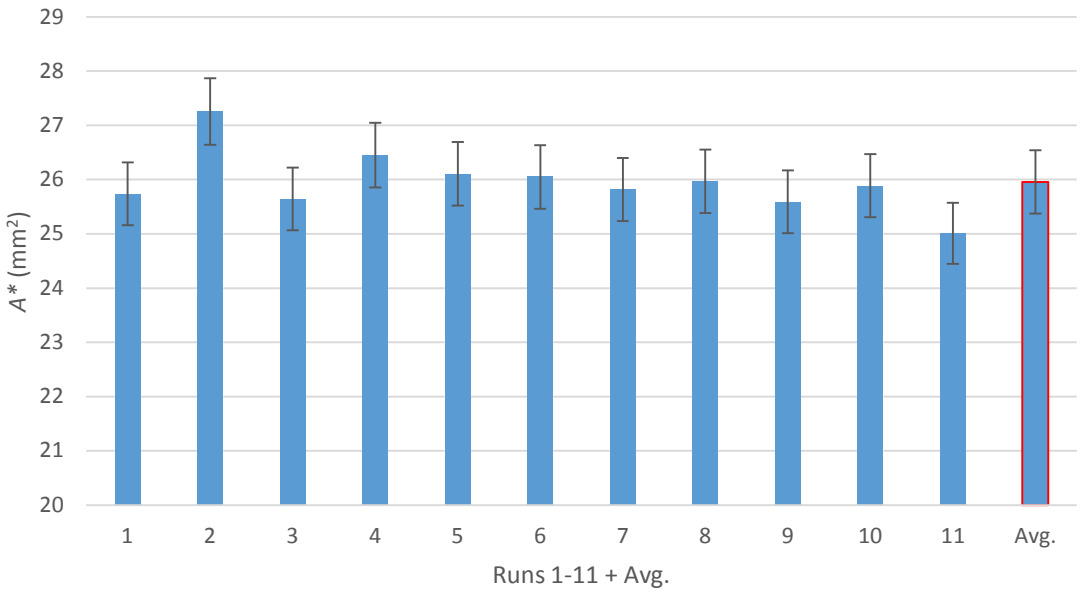

Figure 26: Calculated *A for fuel manifold vs. run. Includes 11 test runs and the average outlined in red. Average valve is 25.96 mm^2 with error bars of ±2.25%**

In Figure 27 the calculated *A** is shown for each test run can be seen along with the calculated error for the oxidizer manifold pair. The average of these values is taken as the true value and has a valve of 47.79 mm^2.

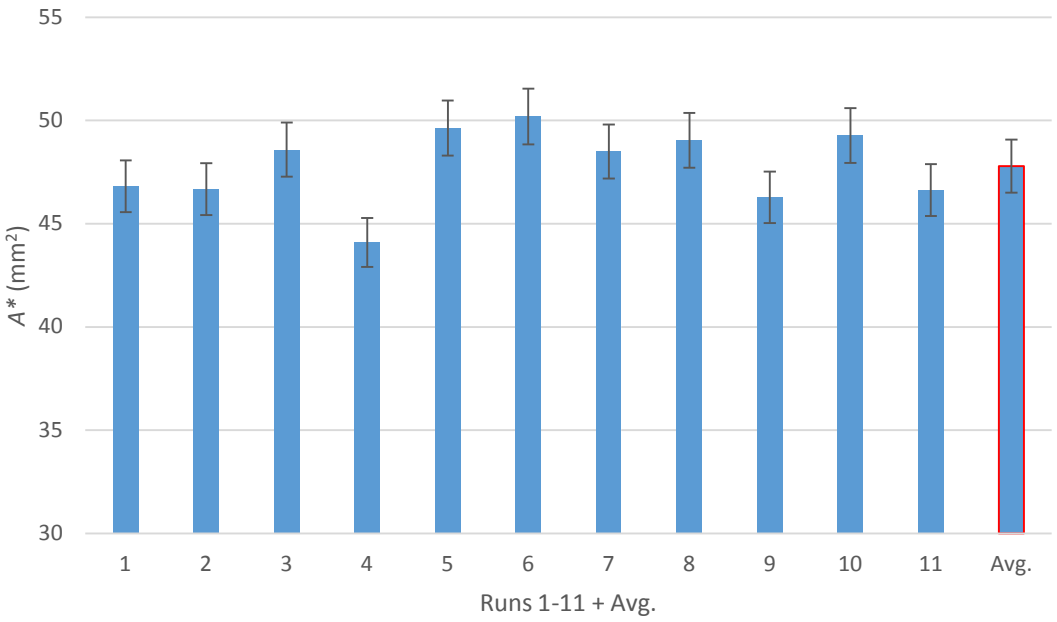

Figure 27: Calculated *A for oxidizer manifolds vs. run. Includes 11 test runs and the average outlined in red. Average valve is 47.79 mm^2 with error bars of ±2.69%**

Wave velocity

In Figure 28, Figure 29, and Figure 30, the wave velocities are shown vs. the time after the data collection was triggered. This data set is for the single shot run with the IP section is position 4. All runs were done with a mixture of methane and oxygen with an Φ between 0.94 and 1.08. The theoretically expected wave velocity was 2389 m/s while all calculated velocities are either 2540 m/s or 2391 m/s. The DAQ was running at 200 kHz. The average wave velocity for all the runs at position 4 was 2512 m/s.

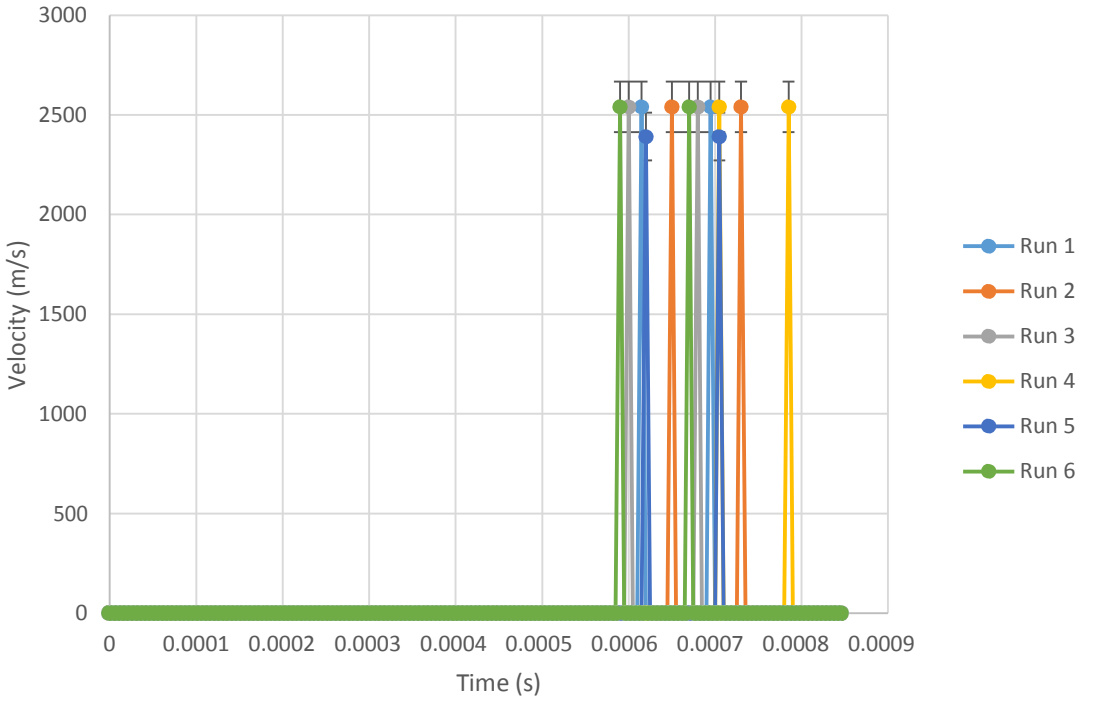

Figure 28: Detonation wave velocity vs. time, runs 1-6. All runs taken with $0.94 \geq \Phi \geq 1.08$ and IPs in position 4.

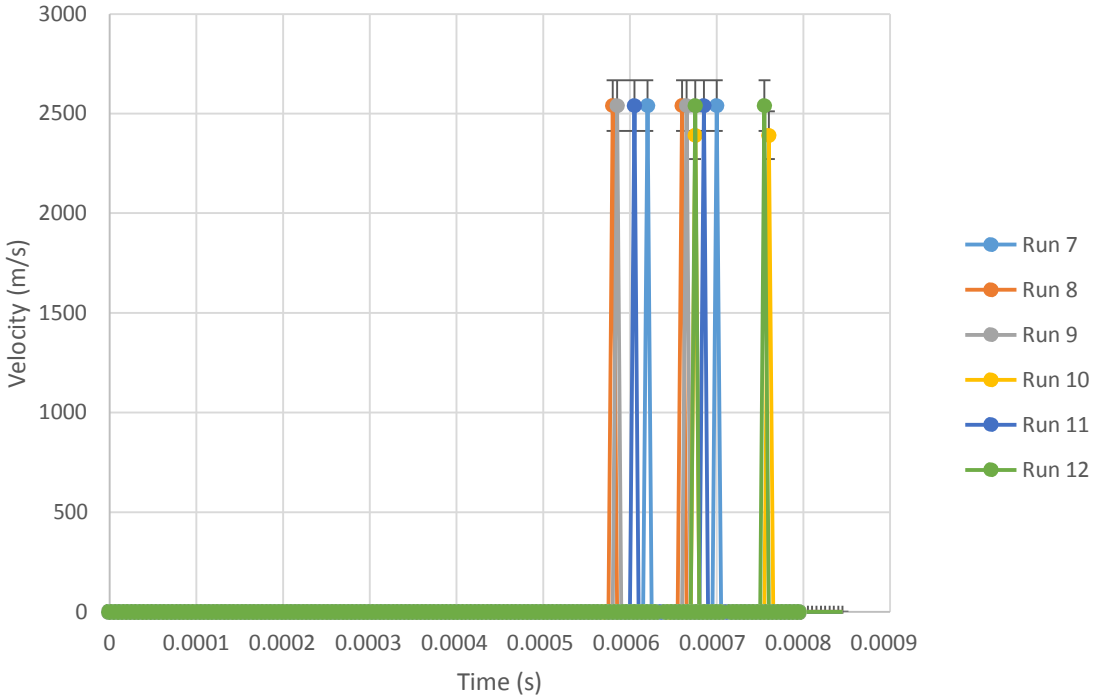

Figure 29: Detonation wave velocity vs. time, runs 7-12. All runs taken with $0.94 \geq \Phi \geq 1.08$ and IPs in position 4.

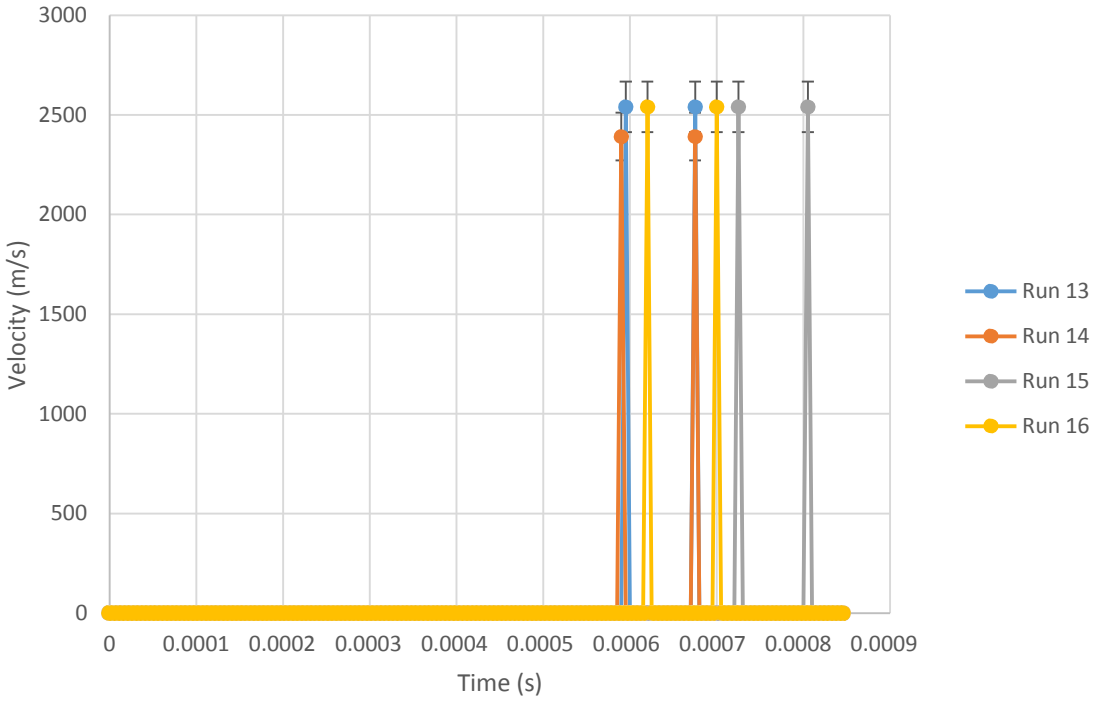

Figure 30: Detonation wave velocity vs. time, runs 13-16. All runs taken with $0.94 \geq \Phi \geq 1.08$ and IPs in position 4.

Figure 31 is raw data from the first run and is generally representative of the raw data. Figure 32 is a close up of the raw data from the fourth run and more easily shows the sudden change in excitation due to the heavily ionized products following a detonation combustion front. Figure 33 is a close up of the IP output during a failure to detonate which can be readily distinguished from a successful detonation.

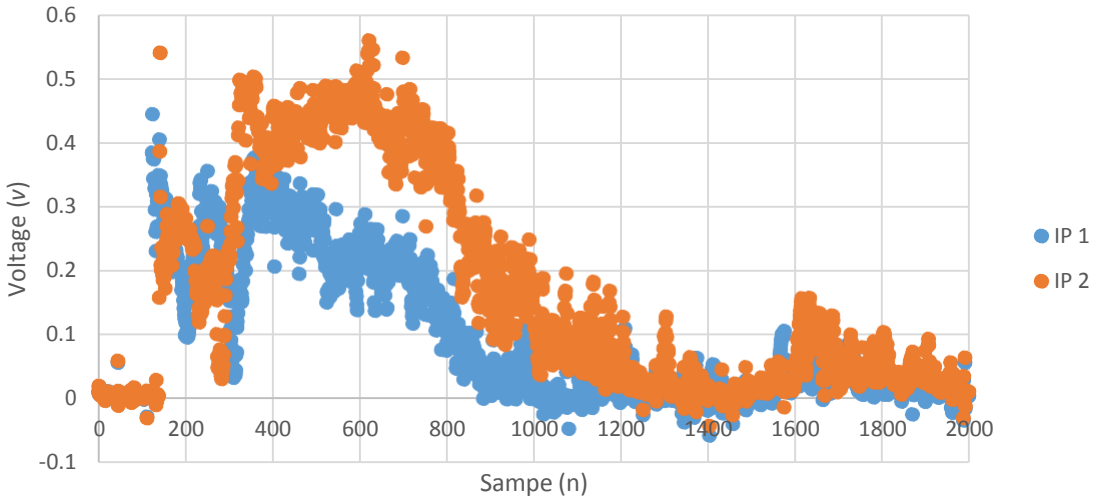

Figure 31: Voltage vs. sample raw data, run 1. Taken with Φ = 1.08 at 200 kHz.

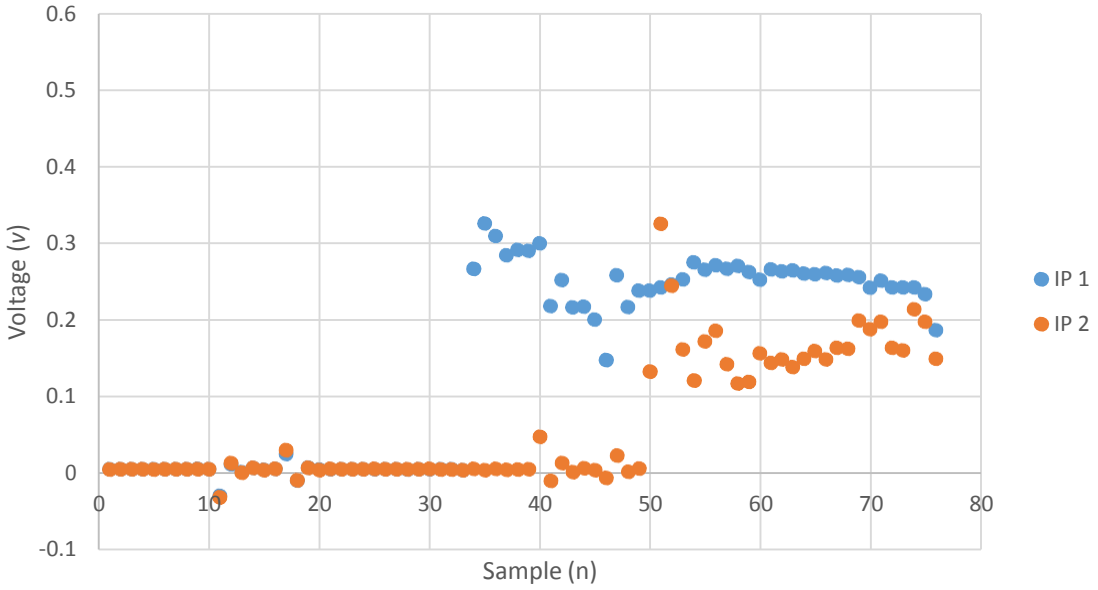

Figure 32: Voltage vs. sample close up of IP excitation during run 4. Taken with Φ = 1.08 at 200 kHz.

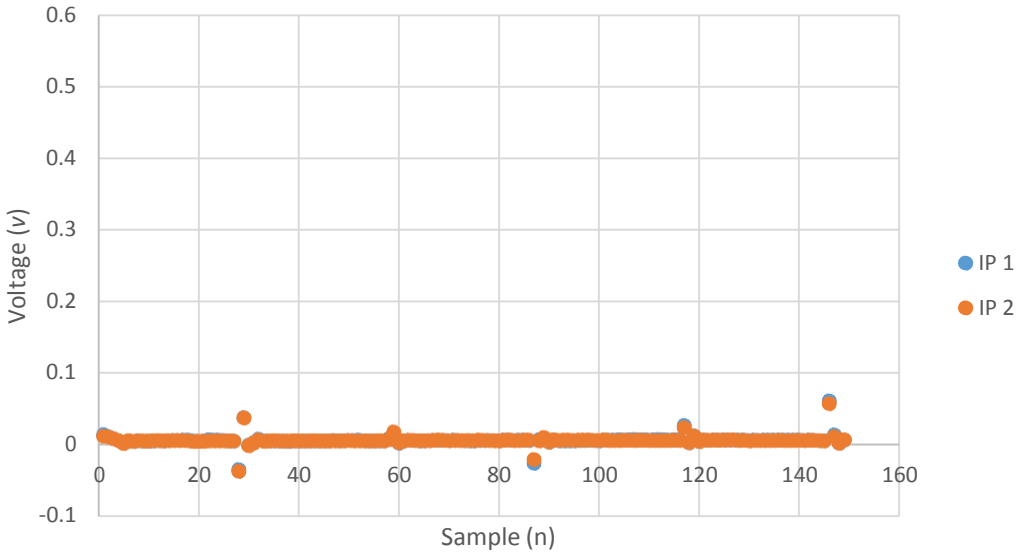

Figure 33: Voltage vs. sample close up of IP excitation during a detonation failure. Taken with Φ = 1.00 at 200 kHz.

The data output for the cyclic tests closely resembles what has already been show for the single shot testing. The completed test matrix can be seen in Table 6. It shows the non-dimensional ratio of the measured detonation wave velocity and the expected detonation wave velocity. It is noteworthy that regardless of the frequency that the PDE was operated at or with the variations in Φ that the velocity ratio at any position only varied within the calculation error of $\pm 6.25\%$.

Table 6: Completed test matrix. The first IP in position 1 is 6" from the ignition source, 18" in position 2, 30" in position 3, and 42" in position 4.

IP Section Position	*Fuel*	*Oxidizer*	*Φ*	*f (Hz)*	*[illegible]*
1	CH_4	O_2	0.94-1.08	1.5, 10, 20	0.85, 0.895
2	CH_4	O_2	0.94-1.08	0.25, 0.5, 1, 1.25, 1.5	0.895, 0.945
3	CH_4	O_2	0.94-1.08	0.25, 0.5, 1, 1.25, 1.5	0.945, 1
4	CH_4	O_2	0.94-1.08	N/A	1, 1.06

High speed video was taken during some of the testing. Figure 34 shows a typical exhaust jet from a successful detonation while Figure 35 shows the typical exhaust flame of a failure to detonate.

Figure 34: Black and white photo of exhaust from a successful detonation.

Figure 35: Black and white photo of exhaust from a failed detonation.

Chapter 6: Conclusions and Recommendations

Conclusions

This work designed, fabricated, and tested a PDE for use as a laboratory test bed. Every physical system was designed from scratch with modularity and ease of alteration in mind as was evident during testing when the IP section position was changed. In addition, it can be seen that the PDE is able to achieve detonation in both single shot and cyclic operation.

Upon inspection of the raw data it can be seen that the detonation wave noticeably excites the IPs which leads to the sharp rise in voltage easily detected above the noise floor. However, during a deflagration event the noise floor is all that can be seen in the recorded samples. In addition, the manifolds and injectors worked quite well during the testing although the variation in Φ appears to come from the pressure regulators.

The wave velocities from all runs are very reasonable with some recorded velocities being within 2 m/s of the expected velocity for a methane-oxygen mixture as can be seen in Table 1. In addition, all velocities when the IP section is in position 3 and 4 are within the expected velocity when error is considered. The velocities recorded at these positions above and below the expected value are possibly from the frequency that the DAQ was set at and with an increase in sampling frequency the velocity values would likely more closely approach the expected value with the decrease in error.

With the IP section in position 1 and 2 the recorded velocity is below the expected but much greater than CJ deflagration. Since ionization is present that can excite the IPs there is detonation present. Although, since the velocity is an average between two points it is possible that separate detonations are present that have not coalesced into a single detonation front which could account for sub CJ velocity.

Recommendations

Generally speaking the objectives of the project were accomplished. However, there is always room for improvement and several areas in particular which would benefit from changes. In particular, the manifold exit on the oxidizer side appears to limit the flow capability of those manifolds. This is likely due to the large restriction that is the one-way check valve. If the paired oxidizer manifolds were separated and the inlet on the head altered to accept this change the same protection from back flow could be assured as well as the associated increase in potential flow.

Another recommendation would be searching for a more elegant control and DAQ solution. Particularly, a combined solution. The necessary evil that was to separate the two is good due to the fact that the current DAQ has very poor performance related to precision timing. However, the separation necessitates the use of more components and wiring, and a slightly lengthier setup time and procedure. It also requires two different types of programming be known to those who would use the PDE.

In addition to alterations to the DAQ, during testing the limitations of the DAQ software and how it interfaces with a computer became very apparent. In particular, with the instabilities mentioned in the Results section. A more stable DAQ is attractive due in large part from a material usage perspective. With the instabilities present it will take more experimental runs, with the associated usage of fuel and oxidizer, to acquire the same number of results.

Tied into the issue with the DAQ is data verification. Currently the data is collected only by IPs and validation done via comparison to reported values of other research or other resources. As has been mentioned in meetings, something such as a

Schlieren system would be extremely useful to future research with the PDE. Due to the PDE's modular design the implementation of the system would not be permanent or too difficult to arrange but would allow a means of verifying results without relying on other resources as well as potentially giving more insight into why potential differences might occur.

An improvement that would be a fundamental addition to the PDE would be the inclusion of cell size monitoring. A variety of other modules have been discussed and several already designed. As cell size is an important and fundamental constraint affecting PDE's it should also be monitored and compared. This is also particularly important as there is a relative dearth on reported cell sizes as parameters are changed.

Regardless of all this, it should be kept firmly in mind that these recommendations are optional as the PDE demonstrated detonation and successful operation in both single shot and cyclic modes. These recommendations would simply make its operation go more smoothly or improve its potential performance.

References

1. Roy, G. D., Frolov, S. M., Borisov, A. A., & Netzer, D. W. (2004). Pulse detonation propulsion: challenges, current status, and future perspective. *Progress In Energy & Combustion Science, 30*(6), 545-672. doi:10.1016/j.pecs.2004.05.001
2. Farokhi, Saeed. *Aircraft Propulsion, 2nd Edition, 2nd Edition*. Wiley-Blackwell, 2014-08-05.
3. Rodriguez, J. (2005). Investigation of Transient Plasma Ignition for a Pulse Detonation Engine, *Naval Postgraduate School*
4. Frolov, S. M., Aksenov, V. S., Gusev, P. A., Ivanov, V. S., Medvedev, S. N., & Shamshin, I. O. (2014). Zel'Dovich thermodynamic cycle and perspectives of its application in chemical ramjet and rocket propulsion. *Center for Pulse Detonation Combustion*
5. Fickett, W., Davis, W. C. (1979). Detonation: Theory and Experiment. Mineola, NY: Dover
6. Ramamurthi, K. (2014). Detonations: Calculation of Chapman Jouguet Velocities, ZND Structure [.flv]. Retreived from http://nptel.ac.in/courses/112106177/26
7. Bussing, T., Pappas, G. (1994). An Introduction to Pulse Detonation Engines. *AIAA*
8. Valli, D. M., Jindal, T. K. (2014). Pulse Detonation Engine: Parameters Affecting Performance. *Internationl Journal of Innovative Research in Science, Engineering and Technology*, 3(4)
9. Kessler, D.A., Gamezo, V.N., Oran, E.S. (2010). Simulations of flame acceleration and deflagration-to-detonation transitions in methane–air systems, Combustion and Flame, 157(11), 2063-2077

10. Frolov, S. M. (2006). Initiation of strong reactive shocks and detonation by traveling ignition pulses. *Journal Of Loss Prevention In The Process Industries*, *19*(2/3), 238-244. doi:10.1016/j.jlp.2005.04.006
11. Bychkov, V., Akkerman, V., Fru, G., Petchenko, A., Eriksson, L. (2007). Flame Acceleration in the early stages of burning in tubes. *Combustion and Flame*, 150, 263-276
12. Valiev, D. M., Bychkov, V., Akkerman, V., Eriksson, L. (2009). Different stages of flame acceleration from slow burning to Chapman-Jouguet deflagration. Doi:10.1103/PhysRevE.80.036317
13. Khokhlov, A. M., Oran, E. S., Thomas, G. O. (1999). Numerical Simulation of Deflagration-to-Detonation Transition: The Role of Shock-Flame Interactions in Turbulent Flames. *The Combustion Institute*
14. Vadim, N. G., Alexei, M. K., Elaine, S. O. (2001). The influence of shock bifurcations on shock-flame interactions and DDT, *Combustion and Flame*, 126(4), 1810-1826
15. Valiev, D. M., Akkerman, V., Kuznetsov, M., Eriksson, L., Law, C. K., Bychkov, V. (2013). Influence of gas compression on flame acceleration in the early stage of burning in tubes. *Combustion & Flame, 160,* 97-111.
16. Nikitin, V. F., Dushin, V. R., Phylippov, Y. G., & Legros, J. C. (2009). Pulse detonation engines: Technical approaches. *Acta Astronautica*, *64*(2/3), 281-287. doi:10.1016/j.actaastro.2008.08.002
17. Wahid, M., Faiz, M., & Saqr, K. M. (2012). Direct thrust force measurement of pulse detonation engine. *AIP Conference Proceedings*, *1440*(1), 1257-1263. doi:10.1063/1.4704344

18. Asato, K. K., Miyasaka, T. T., Watanabe, Y. Y., & Tanabashi, K. K. (2013). Combined effects of vortex flow and the Shchelkin spiral dimensions on characteristics of deflagration-to-detonation transition. *Shock Waves*, *23*(4), 325-335. doi:10.1007/s00193-012-0430-7

19. UT Arlington Aerodynamics Research Center (2008). Early Pulsed Detonation Engine Mishaps [.flv]. Retrieved from https://www.youtube.com/watch?v=GqLOI3h0DC8

20. Panicker, P. K., Lu, F. K., Wilson, D. R. (2009). Practical Methods for Reducing the Deflegration-to-Detonation Transition Length for Pulse Detonation Engines. *Proceedings of International Symposium on Experimental and Computational Aerothermodynamics of Internal Flows*

21. Yoshida, A., Okuda, Y., Yatsufusa, T., Endo, T., Taki, S., Aoki, S., Umeda, Y. Detontion Properties of Mixed-Fuel-and-Air Gas Mixtures.

22. Finigan, D. J., Dohm, B. D., Mockelman, J. A., & Oehlschlaeger, M. A. (2012). Deflagration-to-detonation transition via the distributed photo ignition of carbon nanotubes suspended in fuel/oxidizer mixtures. *Combustion & Flame*, *159*(3), 1314-1320. doi:10.1016/j.combustflame.2011.09.017

23. Huang, Y. Y., Tang, H. H., Li, J. J., & Zhang, C. C. (2012). Studies of DDT enhancement approaches for kerosene-fueled small-scale pulse detonation engines applications. *Shock Waves*, *22*(6), 615-625. doi:10.1007/s00193-012-0396-5

24. Cooper, M., Jackson, S. I., Lieberman, D., Pintgen, F., Shepherd, J. E., Wintenberger, E. Detonation Initiation, Diffraction, and Engine Component Performance.

25. Veldhuizen, E. M., Rutgers, W. R. (2002). Pulsed positive corona streamer

propagation and branching. *Journal of physics D: Applied Physics*, 35, 2169-2179

26. Cain, R., Browning, P., Huebsch, W., and Wilhelm, J., "Investigation of Small Scale Pulsed Detonation Engines and Feasibility Study for Implementation with Disposable Unmanned Aerial Systems," SAE Int. J. Aerosp. 6(2): 2013, doi:10.4271/2013-01-2304.

Appendix A: Arduino Source Code

Arduino Code

```
#include <PWM.h> //includes the PWM library.
                 //this takes away 1 PWM channel

int i; //general int for monitoring loop iterations
int j; //int for controlling firing loop entrance
int k; //int for controlling control loop entrance
int X; //int for checking inputs
int pos; //int for checking whether possitie or negative
int timingCheck; //int used to verify the device timing and
                 //desired frequency are possible

int iterations; //desired amount of iterations for the run
float deviceFREQ; //desired frequency of the void loop and
                  //therefore, device, in Hz
float deviceFREQwhole; //adds the whole side of the frequncy
float deviceFREQfraction; //adds the potentially fractional
                          //side of the frequency
float num; //numerator for fraction
float den; //denominator for fraction

int oxy = 6; //sets up pin 6 for oxidizer signal output
int fuely = 7; //sets up pin 7 for fuel signal output
int sparky = 8; //sets up pin 8 for spark signal output
int signaly = 9; //sets up pin 9 to signal data aquisition
                 //unit to record data

int fuelyON; //fuel on time in ms
int sparkyON; //coil charge time in ms, for LS series coil
              //keep at 4ms, spark occurs at end of coil
              //charge
int signalyON; //time, in ms, to keep data aquisition unit
               //recording data

int fuelyDelay; //delays fuel on time, in ms, to create
                //an oxidizer barrier
int sparkyDelay; //delays coil charge time, if
                 //set to zero coil discharges
                 //same time oxydizer and fuel
                 //are turned off
int signalyDelay; //time delay, in ms, before data aquisition
                  //is turned on after coil is given signal
```

```
            //to discharge (spark occurs)

int ON = 255; //sets 8-bit duty cycle to 0%
int OFF = 0; //sets 8-bit duty cycle to 0%

int32_t frequency = 10000; //pin timing frequency (in Hz)



//------------------------------------------------------------------------------------------------------------
----------------------------------
//------------------------------------------------------------------------------------------------------------
----------------------------------
//------------------------------------------------------------------------------------------------------------
----------------------------------
//------------------------------------------------------------------------------------------------------------
----------------------------------

void setup ()
{
  // put your setup code here, to run once:

  //initializes serial communication
  Serial.begin(9600); //begins serial communications
  //initialize all timers except for 0 to save time keeping functions
  InitTimersSafe();

  //sets the frequency for the specified pin
  bool successOXY = SetPinFrequencySafe(oxy, frequency);
  bool successFUELY = SetPinFrequencySafe(fuely, frequency);
  bool successSPARKY = SetPinFrequencySafe(sparky, frequency);
  bool successSIGNALY = SetPinFrequencySafe(signaly, frequency);

  //if the pin frequency was set successfully, turn pin 13 on
  if (successOXY && successFUELY && successSPARKY && successSIGNALY)
  {
    pinMode(13, OUTPUT);
    digitalWrite(13, HIGH);
  }
  //turns off LED attached to pin 13 and all potential PWM outputs
  else
  {
    pinMode(13, OUTPUT);
    digitalWrite(13, LOW);
    pwmWrite(oxy, OFF);
```

```
  pwmWrite(fuely, OFF);
  pwmWrite(sparky, OFF);
  pwmWrite(signaly, OFF);
  //infinite pin 13 cycling loop if issue detected
  while(1)
  {
    digitalWrite(13, HIGH); //turns LED on pin 13 on
    delay(1000); //wait for desired on time, in ms
    digitalWrite(13, LOW); //turns the LED on pin 13 off
    delay(1000); //waits for desired off time, in ms
  }
}


 i = 1;
 j = 0;
 X = 0;
 deviceFREQwhole = 1;
 deviceFREQfraction = 0;
 deviceFREQ = deviceFREQwhole + deviceFREQfraction;
 iterations = 1;

 fuelyDelay = 0;
 fuelyON = 10;
 sparkyDelay = 0;
 sparkyON = 4;
 signalyDelay = 0;
 signalyON = 0;


Serial.println("PDE timing control.");
Serial.println("THIS PROGRAM REQUIRES INTEGER INPUTS ONLY");
Serial.println("Enter the integer number value corresponding to any below option :");
Serial.println("VALUES MUST BE ENTERED IN THE FORMAT SHOWN.");
Serial.println("Current Values       (1)      About Values              (2)");
Serial.println("PDE Frequency Whole  (3,#)    PDE Frequency Fractional  (4,num,den)
Iterations      (5,#)");
Serial.println("Fuel On Time         (6,#)    Spark On Time             (7,#)       Signal On
Time  (8,#)");
Serial.println("Fuel Delay           (9,#,+)  Spark Delay               (10,#)      Signal Delay
(11,#)");
Serial.println("                      Repeat Program Introduction (555)");
Serial.println("                      START ITERATIONS           (777)");

}
```

```
//-------------------------------------------------------------------------------------------------------------
-----------------------------------
//-------------------------------------------------------------------------------------------------------------
-----------------------------------
//-------------------------------------------------------------------------------------------------------------
-----------------------------------
//-------------------------------------------------------------------------------------------------------------
-----------------------------------
void loop()
{
  // put your main code here, to run repeatedly:
k=0;
while (Serial.available() > 0 && k==0)
{
  X=Serial.parseInt();
  if (X==1) //displays current values
  {
Serial.print("Below are current values:\n");
Serial.print("PDE Frequency (Hz)    : "); Serial.println(deviceFREQ);
Serial.print("Iterations to run (#)   : "); Serial.println(iterations);
Serial.print("Fuel On Time (ms)       : "); Serial.println(fuelyON);
Serial.print("Spark On Time (ms)     : "); Serial.println(sparkyON);
Serial.print("Signal On Time (ms)    : "); Serial.println(signalyON);
Serial.print("Fuel Delay (ms)         : "); Serial.println(fuelyDelay);
Serial.print("Spark Delay (ms)       : "); Serial.println(sparkyDelay);
Serial.print("Signal Delay (ms)      : "); Serial.println(signalyDelay);
Serial.println("Enter a new value : ");
k=1;

  }
  else if (X==2) //displays the about info of each value
  {
Serial.println("PDE Frequency Whole       : The whole number for Frequency.");
Serial.println("PDE Frequency Fractional  : The fractional number for Frequency.
num/den");
Serial.println("Iterations                : How many cycles the PDE will attempt.");
Serial.println("Fuel On Time              : How long, in ms, the fuel valves will open.");
Serial.println("Spark On Time             : Controls coil dwell time, keep at 4ms for truck
coil.");
Serial.println("Signal On Time            : How long, in ms, the DAQ signal will be on.");
Serial.println("Fuel Delay                : Controls delay between fuel and oxidizer, in ms,");
Serial.println("                        + values mean the fuel valves open after the oxidizer.");
Serial.println("                        Enter a 1 for a possitive value and 0 for negative.");
```

```
Serial.println("Spark Delay              : Controls the delay between fuel and oxidizer
valves");
Serial.println("                         closing and spark occuring, in ms, + values mean
spark");
Serial.println("                         occursafter valves close.");
Serial.println("Signal Delay             : Controls the timing of the DAQ signal, in ms, +
values");
Serial.println("                         mean the signal comes after the spark.");
Serial.println("Enter a new value : ");
k=1;
  }

  else if (X==3) //sets the device frequency
  {
deviceFREQwhole=Serial.parseInt();
deviceFREQ = deviceFREQwhole + deviceFREQfraction;
Serial.print("PDE Frequency (Hz) : "); Serial.println(deviceFREQ);
Serial.println("Enter a new value : ");
k=1;
  }

  else if (X==4) //sets the device frequency
  {
num=Serial.parseInt();
den=Serial.parseInt();
deviceFREQfraction = num / den;
deviceFREQ = deviceFREQwhole + deviceFREQfraction;
Serial.print("PDE Frequency (Hz) : "); Serial.println(deviceFREQ);
Serial.println("Enter a new value : ");
k=1;
  }

  else if (X==5) //sets the number of iterations to run
  {
iterations=Serial.parseInt();
Serial.print("Iterations to run (#) : "); Serial.println(iterations);
Serial.println("Enter a new value : ");
k=1;
  }

  else if (X==6) //sets the device frequency
  {
fuelyON=Serial.parseInt();
Serial.print("Fuel On Time (ms) : "); Serial.println(fuelyON);
Serial.println("Enter a new value : ");
k=1;
```

```
  }

  else if (X==7) //sets the Spark on time (coil dwell)
  {
sparkyON=Serial.parseInt();
Serial.print("Spark On Time (ms) : "); Serial.println(sparkyON);
Serial.println("Enter a new value : ");
k=1;
  }

  else if (X==8) //sets the Signal on time
  {
signalyON=Serial.parseInt();
Serial.print("Signal On Time (ms) : "); Serial.println(signalyON);
Serial.println("Enter a new value : ");
k=1;
  }

  else if (X==9) //sets the fuel delay timing
  {
fuelyDelay=Serial.parseInt();
pos=Serial.parseInt();
if (pos==1)
{
}
else if (pos==0)
{
  fuelyDelay=fuelyDelay*(-1);
}
else
{
Serial.println("You entered an incorrect value for + (1 or 0 expected)");
}
Serial.print("Fuel Delay (ms) : "); Serial.println(fuelyDelay);
Serial.println("Enter a new value : ");
k=1;
  }

  else if (X==10) //sets the fuel delay timing
  {
sparkyDelay=Serial.parseInt();
Serial.print("Spark Delay (ms) : "); Serial.println(sparkyDelay);
Serial.println("Enter a new value : ");
k=1;
  }
```

```
  else if (X==11) //sets the fuel delay timing
  {
signalyDelay=Serial.parseInt();
Serial.print("Signal Delay (ms) : "); Serial.println(signalyDelay);
Serial.println("Enter a new value : ");
k=1;
  }

  else if (X==555) //prints the introduction again
  {
Serial.println("PDE timing control.");
Serial.println("THIS PROGRAM REQUIRES INTEGER INPUTS ONLY");
Serial.println("Enter the integer number value corresponding to any below option :");
Serial.println("VALUES MUST BE ENTERED IN THE FORMAT SHOWN.");
Serial.println("Current Values       (1)      About Values              (2)");
Serial.println("PDE Frequency Whole  (3,#)    PDE Frequency fractional  (4,num,den)
Iterations      (5,#)");
Serial.println("Fuel On Time         (6,#)    Spark On Time             (7,#)       Signal On
Time  (8,#)");
Serial.println("Fuel Delay           (9,#,+)  Spark Delay               (10,#)      Signal Delay
(11,#)");
Serial.println("                     Repeat Program Introduction (555)");
Serial.println("                     START ITERATIONS            (777)");
  }

  else if (X==777) //starts the cycles using commanded values
  {
Serial.println("STARTING PDE");
j=1;
k=1;
  }

  else if (Serial.read() == '\n')
  {
k=1;
  }

}

//-------------------------------------------------------------------------------------------------------
-----------------------------------
//-------------------------------------------------------------------------------------------------------
-----------------------------------
  //checkings to ensure that the desired timing is remotely possible
  //does not take into account signal aquisition
  if (j==1)
```

```
  {
     timingCheck = 1000/deviceFREQ-(fuelyON+fuelyDelay
           +sparkyDelay+signalyON+signalyDelay);
           //the timingCheck equation
  }

  if (1000/deviceFREQ<timingCheck && j==1)
  {
   Serial.println("Desired timing is not possible, please change values such that");
   Serial.println("there are timing overruns for the desired frequency.");
   j=0;
  }

//-------------------------------------------------------------------
  //main loop inside void loop for counting interations
  while (i<=iterations && j==1)
  {
//for no delay between fuel and ozidizer
    if (fuelyDelay==0)
    {
      pwmWrite(oxy, ON);
      pwmWrite(fuely, ON);
      if (sparkyDelay>=sparkyON) //spark timing
      {
         delay(fuelyON);
       pwmWrite(oxy, OFF);
       pwmWrite(fuely, OFF);
       delay(sparkyDelay-sparkyON);
       pwmWrite(sparky, ON);
       delay(sparkyON);
       pwmWrite(sparky, OFF);
      }
      else
      {
         delay(fuelyON-sparkyON+sparkyDelay);
       pwmWrite(sparky, ON);
         delay(sparkyON-sparkyDelay);
       pwmWrite(oxy, OFF);
       pwmWrite(fuely, OFF);
       delay(sparkyDelay);
       pwmWrite(sparky, OFF);
      }
    }

//-------------------------------------------------------------------
//for fuel after oxidizer delay
```

```
    else if (fuelyDelay>0)
    {
     pwmWrite(oxy, ON);
        delay(fuelyDelay);
     pwmWrite(fuely, ON);
     if (sparkyDelay>=sparkyON) //spark timing
     {
        delay(fuelyON);
      pwmWrite(oxy, OFF);
      pwmWrite(fuely, OFF);
      delay(sparkyDelay-sparkyON);
      pwmWrite(sparky, ON);
      delay(sparkyON);
      pwmWrite(sparky, OFF);
     }
     else
     {
        delay(fuelyON-sparkyON+sparkyDelay);
      pwmWrite(sparky, ON);
        delay(sparkyON-sparkyDelay);
      pwmWrite(oxy, OFF);
      pwmWrite(fuely, OFF);
      delay(sparkyDelay);
      pwmWrite(sparky, OFF);
     }
    }

//-------------------------------------------------------------------
//for oxidizer starting after fuel valve is opened fuel delay
    else if (fuelyDelay<0)
    {
     pwmWrite(fuely, ON);
     delay(fuelyDelay*(-1));
     pwmWrite(oxy, ON);
          if (sparkyDelay>=sparkyON) //spark timing
     {
        delay(fuelyON);
      pwmWrite(oxy, OFF);
      pwmWrite(fuely, OFF);
      delay(sparkyDelay-sparkyON);
      pwmWrite(sparky, ON);
      delay(sparkyON);
      pwmWrite(sparky, OFF);
     }
     else
     {
```

```
        delay(fuelyON-sparkyON+sparkyDelay);
       pwmWrite(sparky, ON);
        delay(sparkyON-sparkyDelay);
       pwmWrite(oxy, OFF);
       pwmWrite(fuely, OFF);
       delay(sparkyDelay);
       pwmWrite(sparky, OFF);
      }
    }
     delay(signalyDelay);
    pwmWrite(signaly, ON);
    delay(signalyON);
    pwmWrite(signaly, OFF);
    delay(timingCheck);
    i=i+1;
  }
i=1; //resets counter for next potential loop

//-----------------------------------------------------------------
//commanded cycle completion notification
    if (j==1)
    {
    Serial.println("Commanded cycles completed, enter new value:");
    j=0;
    }
}
```

Appendix B: Custom Circuitry Details

All custom circuitry was designed to utilize as few parts as possible while being as robust as possible. To do so, all components are rated at least 30% above the expected voltage and power through each component. All resistors are 1% tolerance and 1/8th watt values. All Metal-Oxide-Semiconductor Field-Effect Transistors (MOSFET), Diodes, and Bipolar Junction Transistors (BJT) are all Logic Level (5 v or less to activate) and rated at or above 30 v. Where pertinent, component part numbers were listed. Otherwise, the component values are listed. In each section are figures which include the populated board, board layout, component value listing, and schematic. Figure 36 though Figure 41 show some of the details or each particular part.

PWM Controller Side Board

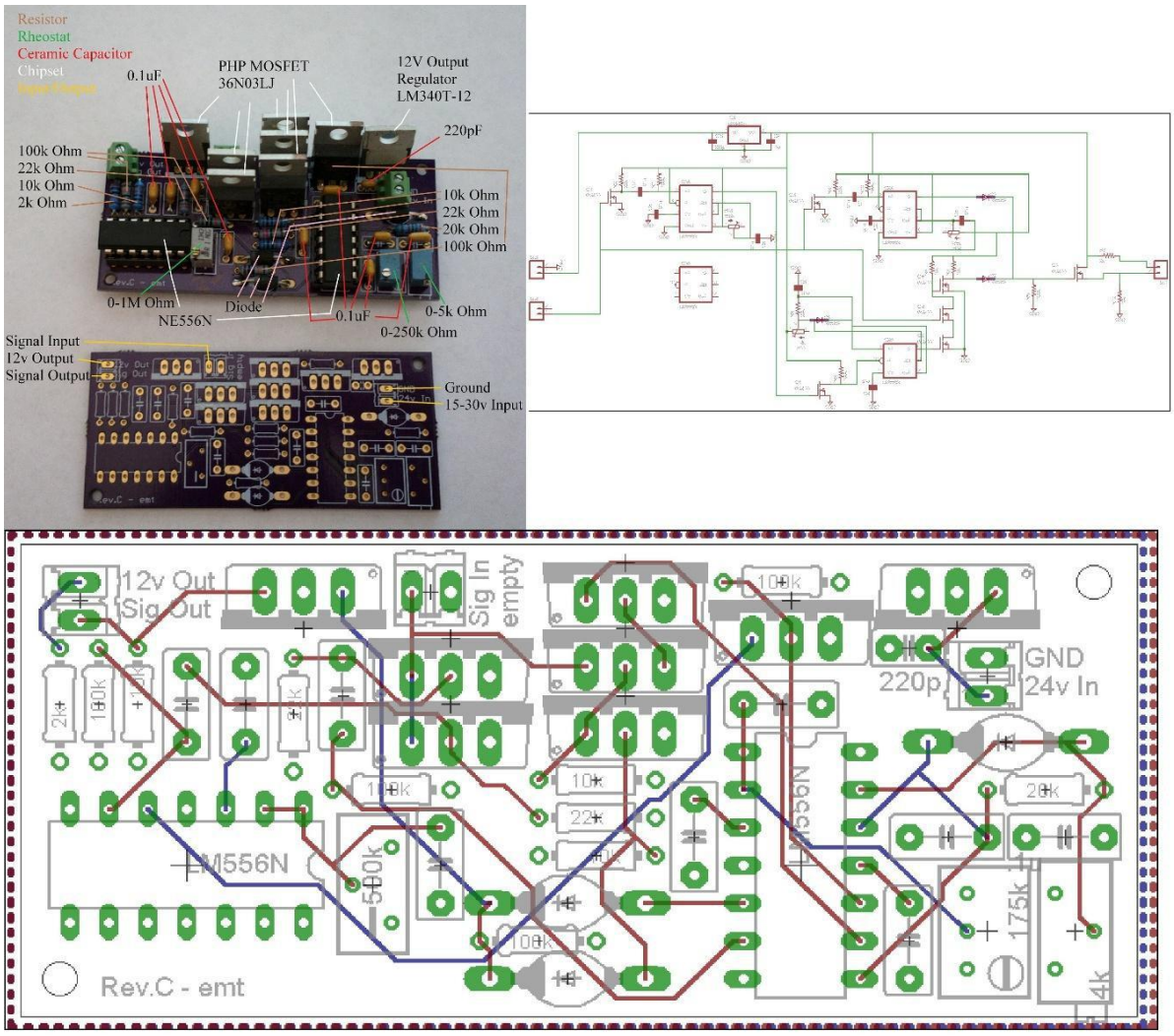

Figure 36: PWM control circuit details. Populated board, bare board, board layout, and schematic.

PWM Switching Side Board

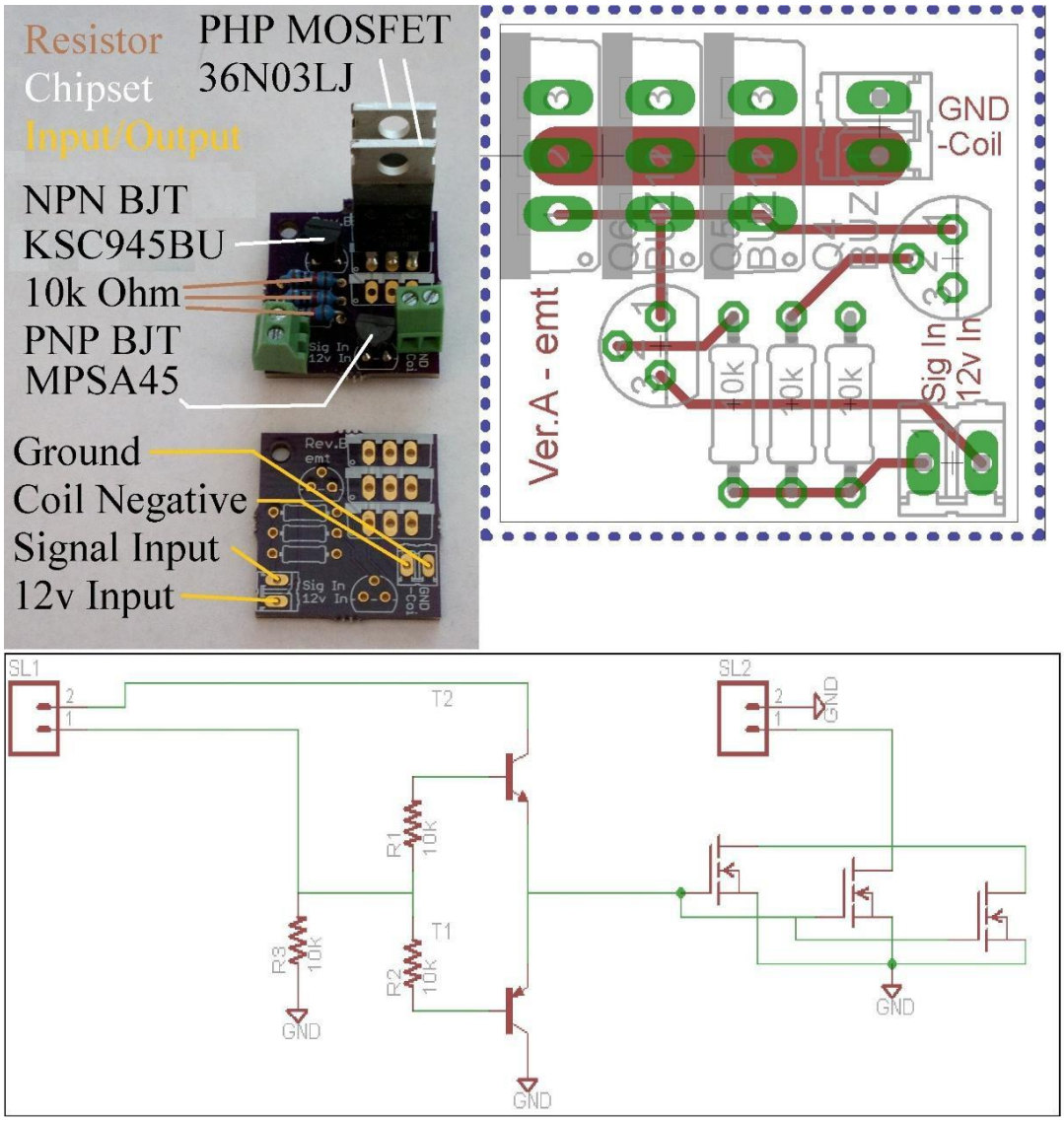

Figure 37: PWM switch circuit details. Populated board, bare board, board layout, and schematic.

Ionization Probe Board

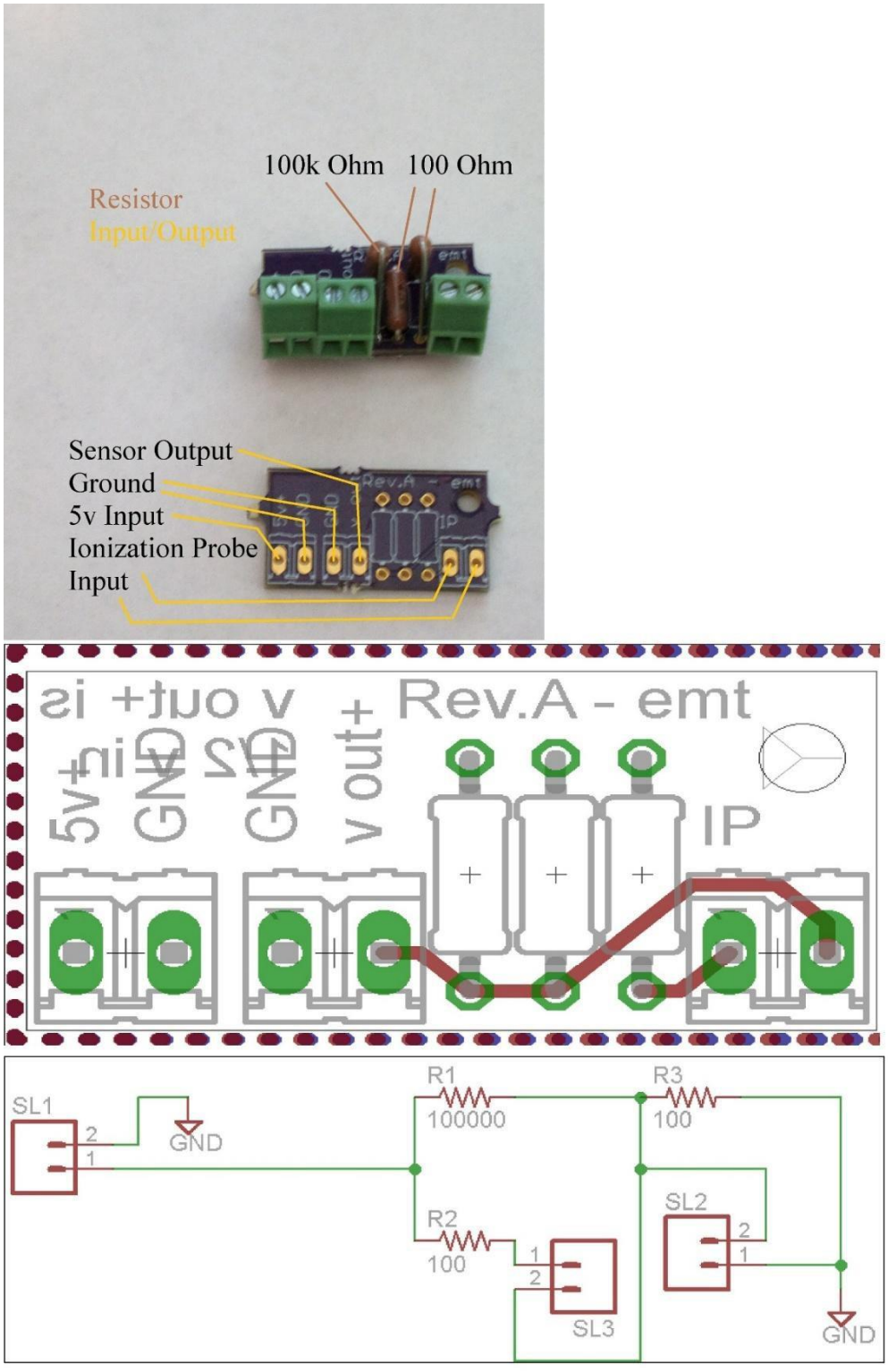

Figure 38: Ionization Probe circuit details. Populated board, bare board, board layout, and schematic.

Pressure Transducer Board

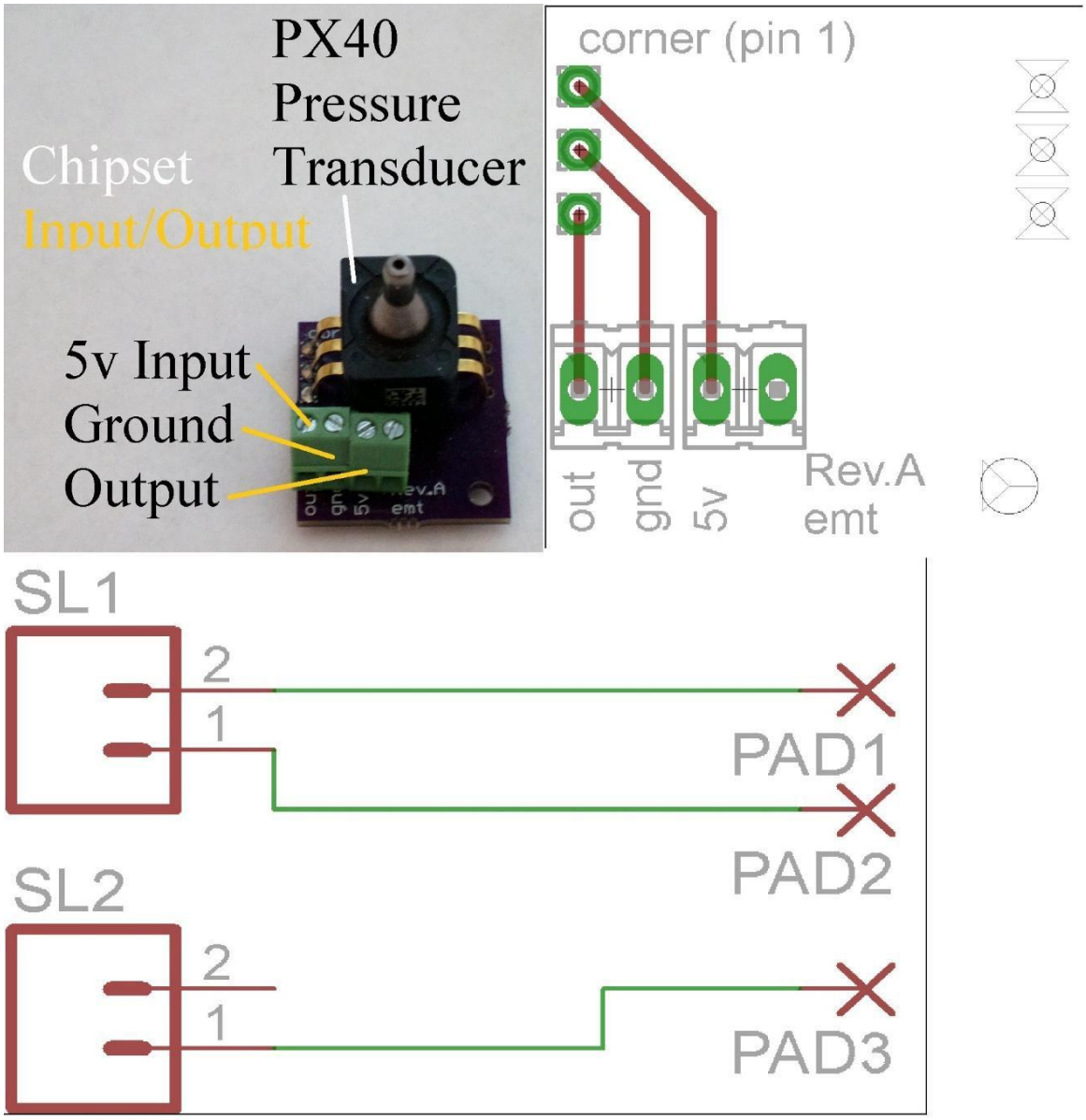

Figure 39: PX40 pressure transducer details. Populated board, board layout, and schematic.

Current Sensor Board

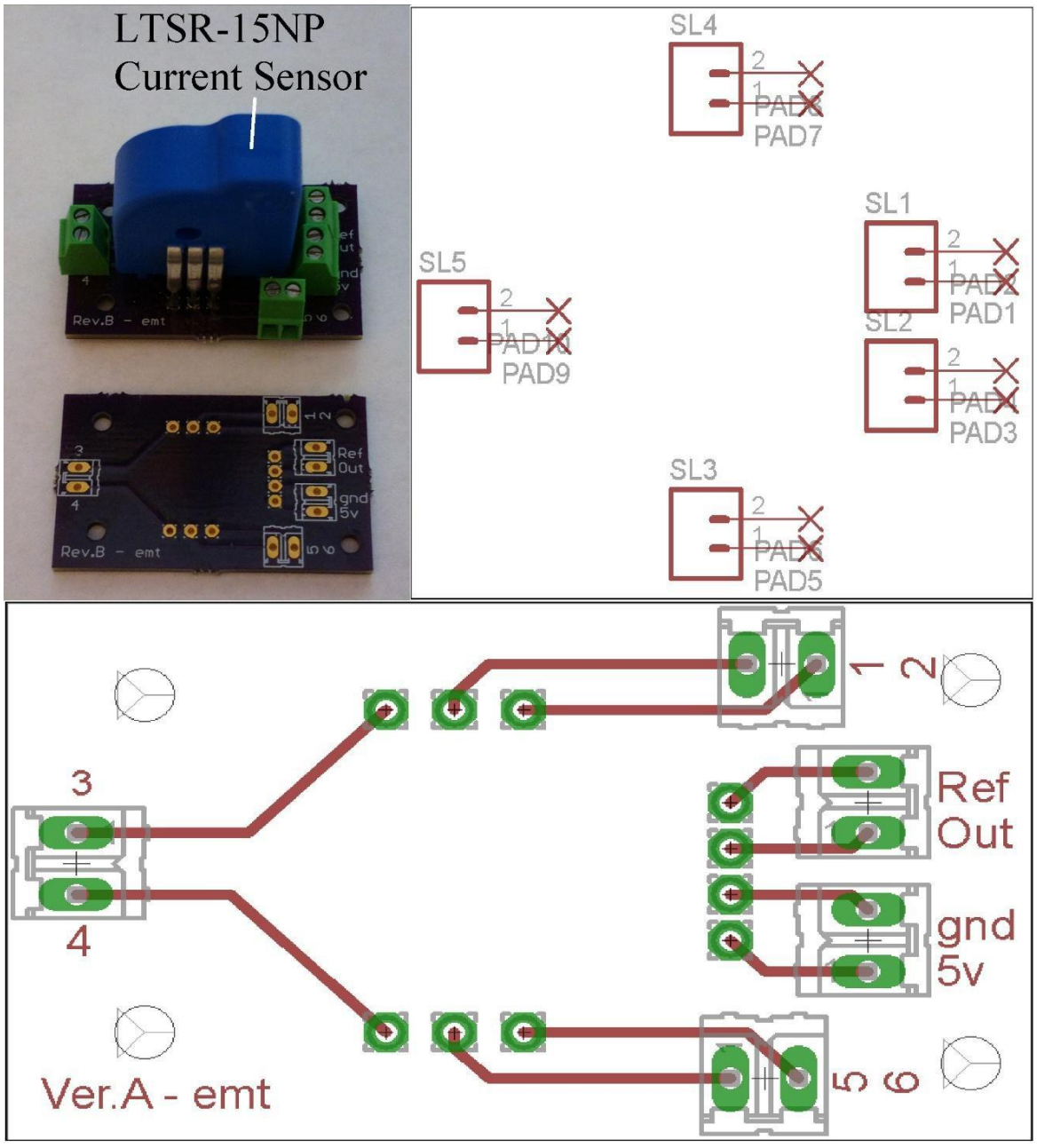

Figure 40: Current sensor board details. Populated board, bare board, board layout, and schematic.

Generic Power Supply Board

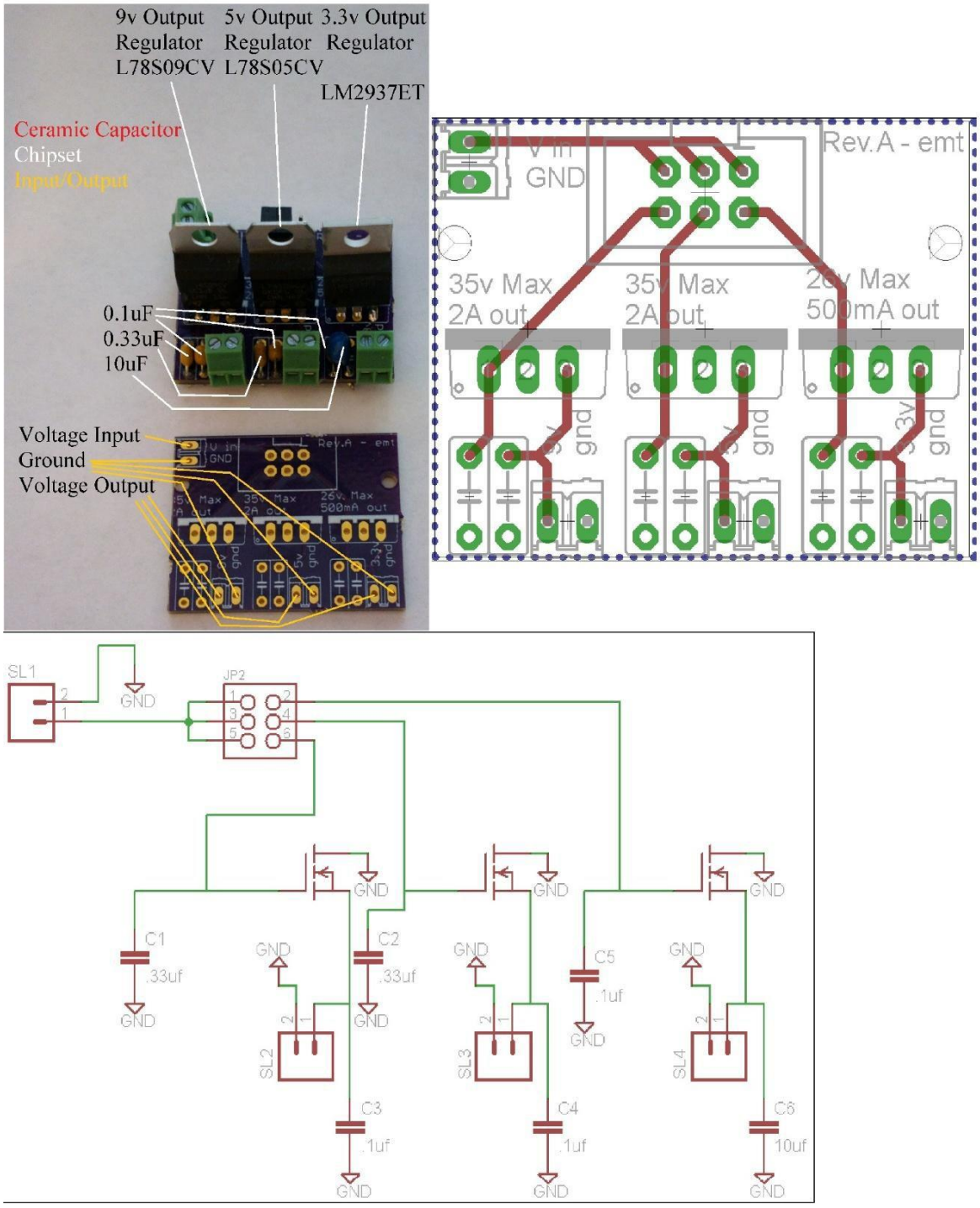

Figure 41: Power supply board details. Populated board, bare board, board layout, and schematic.

Appendix C: Setup and Operating Procedure

The PDE was designed to be as simple to setup and operate as possible. In general, the PDE simply needs 24 v from two automotive batteries, fuel and oxidizer to the appropriate manifold, and a computer which can connect to the Arduino which controls the injectors and ignition source. In Figure 42, is a schematic that shows the basic layout and connections of each component for basic operation.

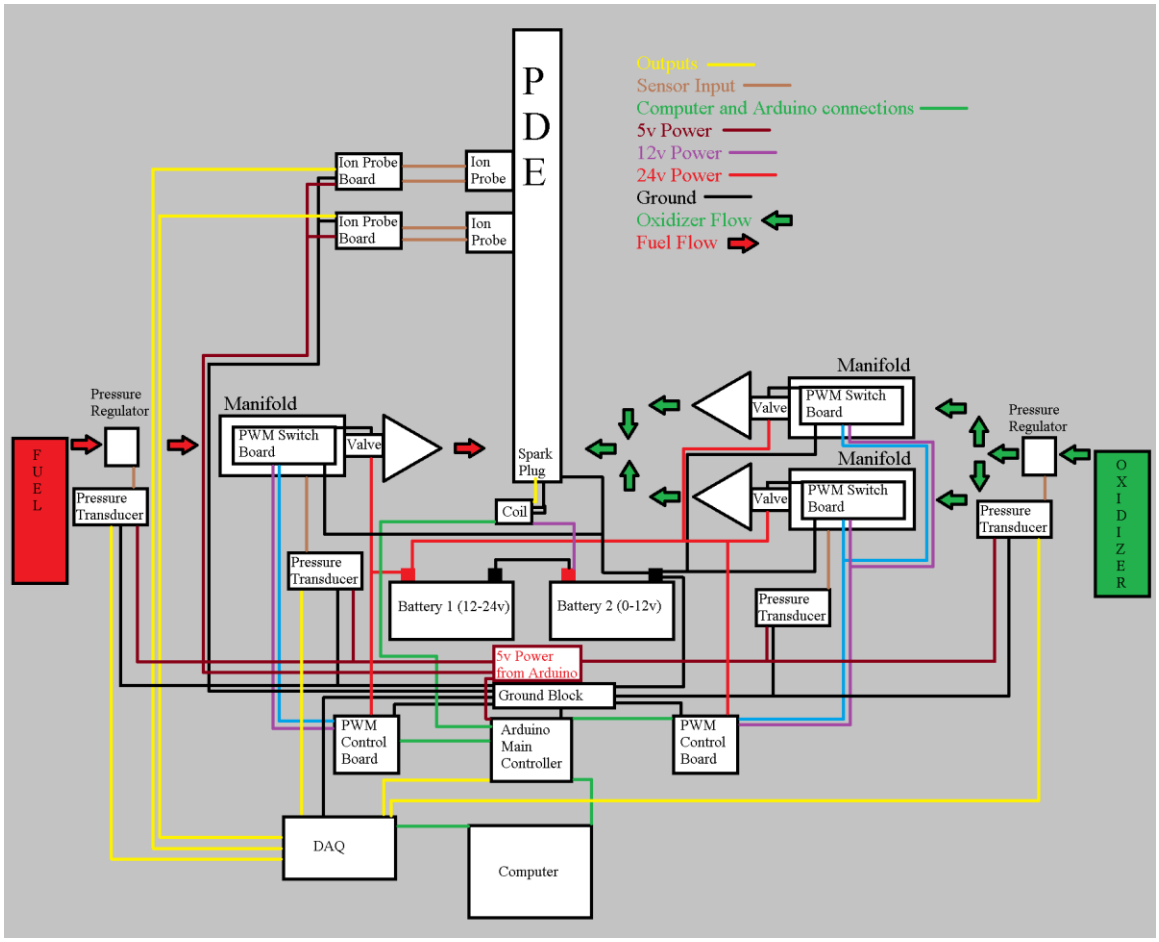

Figure 42: PDE layout.

The PDE has a variety of components and junctions as can be seen above. The following will be a description of the general layout of the PDE as shown in Figure 42. It should be noted that this will only go over the physical layout as the Arduino

programming which controls the PDE's operation is very simple and even has a help feature programmed into it should there be any confusion.

Computer

The computer is connected via USB to both the DAQ and Arduino. It is required that the computer be able to interface directly with the Arduino though its Integrated Development Environment (IDE) such that it can be controlled via the built in serial interface. Issues connecting to the IDE are not within the scope of this paper and help should be sought in the IDE manual if problems occur. However, it is noted that the majority of problems that occur are from the incorrect specification of either BAUD rate or communication (COM) port.

Arduino

An Arduino was chosen to control the PDE due to its excellent timing. It has the further benefit of being relatively simple to program, has a good 5 v output, and is expandable. Keep in mind that the Arduino output can be changed and as such, which output wires go where should be inspected in the programming. This is easily done in the IDE before the serial connection is even opened.

The Arduino has more than a dozen Digital Input Output (DIO) which can be precisely controlled to produce the square wave logic level input that the PWM controller expects. With the current programming all inputs are through the IDE serial connection and done in whole numbers. The required format for altering an option is displayed next to the option in brackets.

DAQ

The DAQ is not required to run the PDE with the current setup. However, it does make data collection from running the PDE relatively easy. The DAQ, in general, can be used to display the various outputs from the pressure transducers as well as collect data from the IPs.

Feed and Ignition System

The feed system of the PDE consists of the separate fuel and oxidizer tanks, their respective pressure regulators, the PDE manifolds, injectors, one way check valves, and finally enter the head.

The pressure regulators are fed directly from their respective high pressure tank and able to supply pressures of up to 250 psig. The pressure regulator does **NOT** have an internal relief valve which means that the pressure cannot be relieved simply by turning the adjustment nut down in the case of it being adjusted too high. This was specified such that flammable and potentially harmful fuels would not be carelessly vented to the atmosphere. However, this caries the risk of over pressurization.

Attached to the pressure regulator is a 0-5000 psig pressure transducer used to monitor the tank pressure. The outlet pressure port is plug as that is monitored on the manifolds.

The pressure regulator feeds, via appropriately colored hose (red for fuel, green for oxidizer), into the PDE manifold(s). The manifolds contain 7 injectors each, 7 PWM switching boards, and potentially one 0-150 psig pressure transducer. The fluid flows through the injectors into the converging nozzle, through the one way check valve, and into the PDE head.

The ignition system is an off the shelf automotive unit and expects a 4 ms logic level square wave to charge the coil. Once the square wave is removed the coil discharges through the spark plug.

Wiring

All grounds from the various sensors and controllers should come together at one place before being connected to Battery 2's ground.

The Pressure Transducers all require a 5 v input which is associated with the red wire, ground on the black wire, and output on the green wire.

The PWM switching boards all expect to see a 12 v supply from their respective PWM control board via the red wire with the spade connector. The see the switching signal from the same board via the white wire with the bullet connector. These switching boards control the injectors by switching ground; that is to say they intermittently connect and disconnect the injectors from ground to complete, or not, the circuit. The ground terminal is connected directly to Battery 2's ground.

The PWM control boards expect the full 24 v from both batteries. They too much be grounded at the ground junction block. The voltage input should come from Battery 1's positive terminal. The signal input comes from its respective Arduino DIO. The signal output and 12 v output is described with the PWM switching board.

Each set of injectors gets direct 24 v on their positive side (red wire) from the positive terminal on Battery 1. The negative side is connected to the PWM switching boards –coil terminal.

The coil requires a 12 v power on its red wire connected directly from Battery 2's positive side. Both of its black wires are grounded to the provided ground lug on the head which is in turn grounded to Battery 2's negative terminal. The signal is fed via the appropriate DIO from the Arduino.

General points

In general, Iridium spark plugs should be utilized for the PDE. This is due to their higher oxidation temperature.

The PDE head and body can be removed from each other quickly and easily with either an 11mm or $7/16^{th}$ wrench.

The grounding block for the various sensors is extremely important. Do not forget to utilize it. It is most easily done via a Breadboard. The same Breadboard can be utilized to distribute the Arduino 5 v source as well.

If some issue emergency arises ensure that it is easy to remove the negative terminal from Battery 2. Always ensure a fire extinguisher is handy and that an escape route is open.

Appendix D: Experimental Calibration and Results

Pressure Transducers

There are four pressure transducers associated with the PDE. There are two OMEGA PX40 rated at 0-150 psig and two OMEGA PX613 rated at 0-3000 psig. The literature on the PX613 states that it is calibrated and tested from the manufacture and that it exceeds the specifications and does not need to be recalibrated. From this assurance, as well as the fact that both PX613 will simply be used to monitor the high pressure tanks, a simple linear equation is derived to translate the PX613s voltage output and to a pressure and is shown in Equation 7.

$$P(v) = 750v - 750v_{0\square\square\square\square} \quad \textbf{Eqn. 7}$$

The PX40 does not have this assurance and was tested to verify its accuracy, zero, and repeatability. Both PX40s were tested with a currently in calibration OMEGA DPG4000 series unit. Each PX40 was tested 10 times at 0 psig, 5 psig, and 9 psig and the voltage output recorded. The testing was done from 0 psig to the specified pressure, data recorded, then the pressure was released. For the 0 psig testing the PX40 was pressurized to an arbitrary pressure then the pressure was released and the voltage output recorded. Both units preformed identically and showed no variance in output across the tested pressures.

When the data was plotted it was found that the goodness of fit (R^2) was indistinguishable from 1. This means that it the linearity of each sensor is very good and that it would not be unreasonable to extrapolate the sensors output to its full range. The best fit line from this data is shown in Equation 8. However, if the setup is not exactly the same there may be some bias introduced from ground offset. Taking this into account

gives rise to Equation 9 which scales the y-intercept by the ratio of the calibration 0 psig voltage output and the current 0psig voltage output. In Figure 43, the data points and trend line can be seen.

$$P(v) = 38.137v - 19.105 \quad \textbf{Eqn. 8}$$

$$P(v) = 38.137v - 38.134v_{0\text{□□□□}} \quad \textbf{Eqn. 9}$$

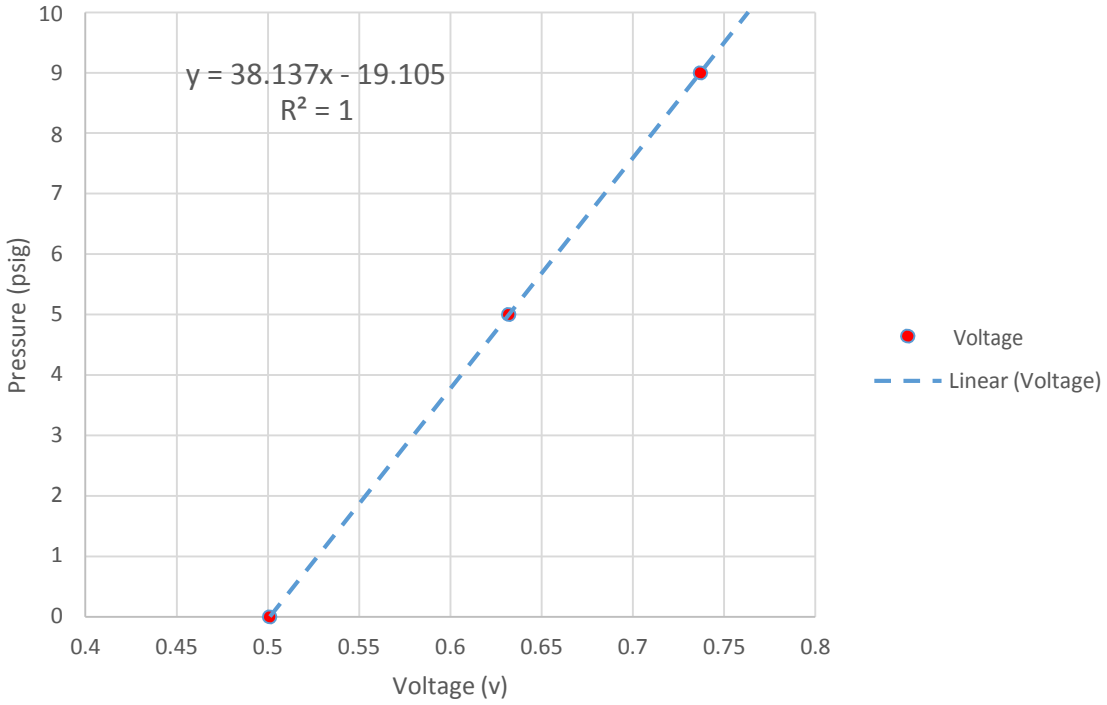

Figure 43: Graph showing Pressure vs. Voltage Output during calibration of PX40 Pressure Transducer. Dashed line is extrapolated trend line.

Manifold *A** Calculation

This calculation is very important, as discussed previously in Chapter 4. Also in Chapter 4 is the general method by which the data was collected. The analysis of the data was simplified by usage of a form of the Ideal Gas Law, Equation 10. The Ideal Gas Law can be utilized in this case as its Z factor is approximately 1. The initial and final mass of

air inside the manifolds was monitored calculated before the injectors were opened and then after they were opened for 200 ms. In Equation 10, the mass is given by *m* and the volume by *V*.

$$\rho = \frac{m}{R_{air} T} \quad \textbf{Eqn. 10}$$

As the injectors are open the manifold pressure is being monitored by a calibrated pressure transducer. The pressure history is now known. A best fit curve is then applied to the pressure history which gives the pressure as a function of time. Using a manipulation of Equation 6, the A^* can be calculated. The manipulation of Equation 6 is shown in Equations 11-14. In the following Equations C_d is simple a term of gathered constants.

$$\frac{m}{t} = \frac{C_d A^* P_0}{\sqrt{T_0}} \sqrt{\gamma \left(\frac{2}{\gamma+1}\right)^{\left(\frac{\gamma+1}{\gamma-1}\right)}} \quad \textbf{Eqn. 11}$$

$$C_d = \frac{1}{\sqrt{R_{air}}} \sqrt{\gamma \left(\frac{2}{\gamma+1}\right)^{\left(\frac{\gamma+1}{\gamma-1}\right)}} \quad \textbf{Eqn. 12}$$

$$\int_{t_0}^{t_1} \dot{m}\, dt = \int_{t_0}^{t_1} P(t) A^* C_d\, dt \quad \textbf{Eqn. 13}$$

$$A^* = \frac{m_{t_1} - m_{t_0}}{C_d \int_{t_0}^{t_1} P(t)\, dt} \quad \textbf{Eqn. 14}$$

An example of the pressure time history with best fit curve is shown in Figure 44.

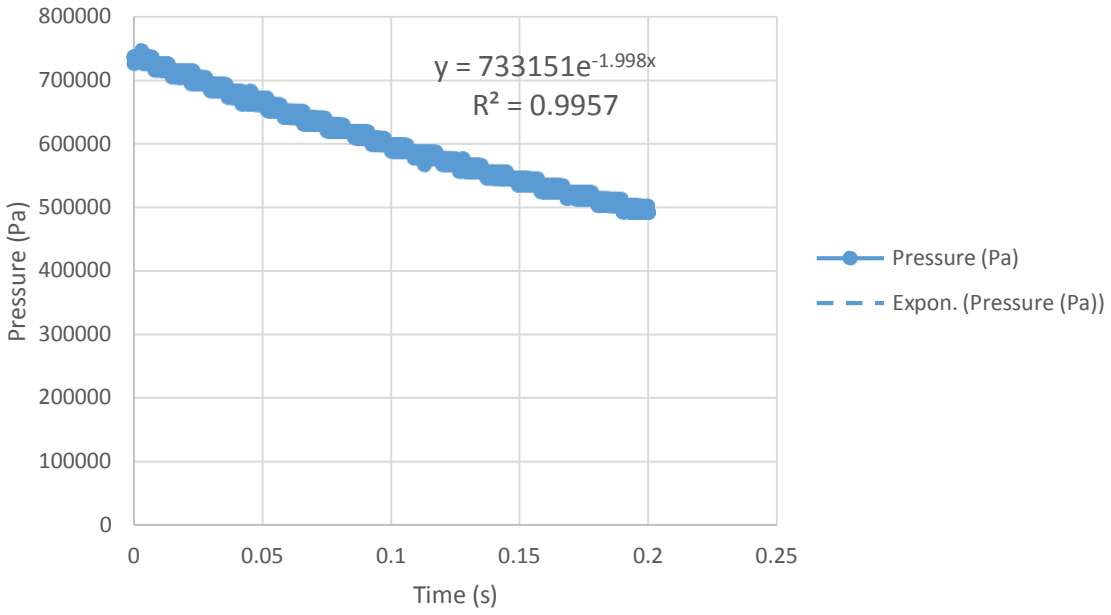

Figure 44: Pressure vs. Time history of the fuel manifold.

During the testing of the manifolds the generic pressure regulator used to feed them gave inconsistent initial pressures. Table 7 and Table 8 shows some of the various values calculated from the testing of the manifolds.

Table 7: Fuel manifold characterization

Trial	*Δ(kg)*	*Best Fit Equation*	R^2	A^* (mm^2)
1	0.007326	$733151e^{-1.998t}$	0.9957	25.7
2	0.007936	$755938e^{-2.082t}$	0.9959	27.3
3	0.007631	$768143e^{-2.02t}$	0.996	25.6
4	0.007631	$745097e^{-2.027t}$	0.9957	26.5
5	0.007326	$724335e^{-2.02t}$	0.9959	26.1
6	0.007326	$724491e^{-1.999t}$	0.9956	26
7	0.007326	$731672e^{-2.01t}$		

8	0.007326	$727457e^{-2.009t}$	0.9955	25.6
9	0.007326	$737673e^{-2.002t}$	0.9957	26
10	0.007326	$730170e^{-2.016t}$	0.9958	25.6
11	0.007020	$724541e^{-2.02t}$	0.9956	25.9
Average	0.007409		0.9957	25
Avg. Per Injector	0.001482			25.96 5.19

Table 8: Oxidizer manifolds characterization

Trial	*Δ(kg)*	*Best Fit Equation*	R^2	A^* (mm^2)
1	0.013523	$723106e^{-1.66t}$	0.9902	46.8
2	0.013523	$703316e^{-1.793t}$	0.9905	46.6
3	0.013523	$698123e^{-1.696t}$	0.9905	44.1
4	0.012294	$696599e^{-1.917t}$	0.99	49.6
5	0.013523	$711280e^{-1.786t}$	0.9899	50.1
6	0.014138	$704749e^{-1.795t}$	0.9913	48.5
7	0.013523	$696359e^{-1.785t}$	0.991	49.0
8	0.013523	$696924e^{-1.673t}$	0.9898	46.3
9	0.012908	$694348e^{-1.805t}$	0.9896	49.3
10	0.013523	$691273e^{-1.668t}$	0.9902	46.6
11	0.012908	$723106e^{-1.66t}$	0.9897	47.8
Average	0.013355			47.8
Avg. Per Injector	0.000954			3.41

Appendix E: Error Analysis

Error in pressure and temperature Readings

The majority of the relevant calculations require accurate pressure readings. From the literature it has a maximum error of ±0.15% full scale. Both PX40 units are 150psig.

$$P_{PX40} = (P_{PX40} \pm 0.225)psi$$

$$P_{PX40} = (P_{PX40} \pm 1551)kPa$$

$$\%P_{PX40} = \pm 0.15\%$$

The local pressure is taken with a mechanical dial gauge with 2kPa graduations. For a typical sample:

$$P_{PX40} = (95 \pm 1)kPa$$

$$\%P_{PX40} = 1.58\%$$

The local temperature is also taken with a mechanical dial gauge with 2 ℃ graduations. For a typical sample:

$$T_{PX40} = (299 \pm 1)K$$

$$\%T_{PX40} = \pm 0.334\%$$

Error in calculated wave velocity

The wave velocity is determined by the excitation of ion probes places in the path of the detonation wave and is given by:

$$V_w = \frac{(x_2 - x_1)}{(t - t_1)}$$

2

The distance between the centers of the ion probes was measured with calipers and took three measurements. One to get the overall distance and the other two to verify the nominal diameters of the section they were threaded into.

$$(x_2 - x_1) = (8.755 \pm 0.0005)" - 2[0.755(\tfrac{1}{2}) \pm 0.0005]"$$

$$\%_{\Delta x} = (0.0125 + 0.13 + 0.13)$$

$$\%_{\Delta x} = \pm 0.27\%$$

The probe samples were taken at 200 kHz. Digitized time samples are only assumed to be as certain as half of their sampling rate, this is given by:

$$\left(\frac{n}{f_s} \pm \frac{1}{2f_s}\right) - \left(\frac{n}{f_s} \pm \frac{1}{2f_s}\right)$$

For a typical Δn of 16 the time error is shown:

$$\%_{\Delta t} = \pm 6.25\%$$

All of these errors combine to a maximum likely error shown:

$$\%_{m} = \sqrt{0.27^2 + 6.25^2}$$

$$\%_{m} = \pm 6.26\%$$

Error in calculated injected mass

To determine the mass of air ejected from the manifolds with known initial and final pressure in kPa.

$$m_{inj} = m_1 - m_2 = \left(\frac{V_1}{R_{air} T}\right)(P_{1,inj} + P_{atm}) - \left(\frac{V_2}{R_{air} T}\right)(P_{2,inj} + P_{atm})$$

Where all variables are known, the respective errors are as follows.

$$\%_{V_{inj}} = \frac{\pi d^2}{4} \times \ell =$$

$$\pi(4.26 \pm 0.0005)^2 \times (10.493 \pm 0.0005)$$
$$4$$

The maximum likely error for the fuel manifold volume is given by:

$$\%_{WF_{\square}} = \sqrt{\left(\frac{.0005}{4.26}\right)^2 + \left(\frac{.0005}{0.493}\right)^2}$$

$$\%_{WF_{\square}} = \pm 0.0126\%$$

Similarly, the feed tube connected to the manifold needs to be taken into account.

$$\%_{F_{\square\square\square}} = \frac{\square\square^2 \times \square}{4} = \frac{\square(0.375 \pm 0.0005)" \times (3.75 \pm 0.0005)"}{4}$$

$$= \frac{}{4}$$

$$\%_{WF_{\square}} = \sqrt{\left(\frac{.0005}{0.375}\right)^2 + \left(\frac{.0005}{3.75}\right)^2}$$

$$\%_{WF_{\square}} = \pm 0.134\%$$

The maximum likely error for the assembly is shown by:

$$\%_{WF_{\square}} = \sqrt{0.0126^2 + 0.134^2}$$

$$\%_{WF_{\square}} = \pm 0.135\%$$

The oxidizer manifolds have the same dimensions but there are two connected together, also, the feed tube is approximately five times longer.

$$\%_{\square 2\square\square\square} = \frac{\frac{\square\square^2}{4} \times \square}{4} = \frac{\square(0.375 \pm 0.0005)" \times (18.75 \pm \frac{1}{64})"}{4}$$

$$= \frac{}{4}$$

$$\%_{\square 2\square\square\square} = \sqrt{\left(\frac{.0005}{0.375}\right)^2 + \left(\frac{.0156}{18.75}\right)^2}$$

$$\%_{\square 2\square\square\square} = \pm 0.157\%$$

Taking into account the differences between the two setups the maximum likely error is shown by:

$$\%_{\square 2\square} = \sqrt{0.0126^2 + 0.0126^2 + 0.157^2}$$

$$\%_{\square 2\square} = \pm 0.158\%$$

Upon inspection of the pressure data it was found that the DAQ sometimes collected the data reduced the accuracy of the PX40 such that the error became ±0.8% PS from the

±0.15% FS. Combining all of these errors the mass injected error for each manifold setup is shown by:

$$\text{[illegible]} = \pm 0.811\%$$

$$\text{[illegible]} = \pm 0.815\%$$

Error in calculated *A**

The value of *A** is very important to the PDE as it is the fundamental value that is used in calculations of the injected mass and expected stoichiometry of the mixture. To do so the combined error of the injected mass and pressure were taken into consideration. The injected mass error has already been described. The error in the pressure is described differently.

The pressure term in the *A** calculation is a function. To assess its maximum likely error, for each manifold, the bet fit line with the lowest R^2 was taken as representing the true pressure values. The standard deviation of the difference between the equation and measured values was then taken. A 95% confidence interval was then taken with the lowest pressure. All of these steps were taken to include the greatest error possible in each step.

At the end of this the error from the pressure term is given as:

$$\text{[illegible]} = \left(\frac{9300\text{[illegible]}}{482900\text{[illegible]}}\right) \times 100\%$$

$$\text{[illegible]} = \pm 1.93\%$$

$$\text{[illegible]} = \left(\frac{11980\text{[illegible]}}{493450\text{[illegible]}}\right) \times 100\%$$

$$\text{[illegible]} = \pm 2.43\%$$

The error in the mass of the manifold as well as the pressure term were then combined for the maximum likely error as given by:

$$\text{Error}_{*F} = \sqrt{0.811^2 + 0.811^2 + 1.93^2}$$

$$\text{Error}_{*F} = \pm 2.25\%$$

$$\text{Error}_{*2} = \sqrt{0.815^2 + 0.815^2 + 2.43^2}$$

$$\text{Error}_{*2} = \pm 2.69\%$$